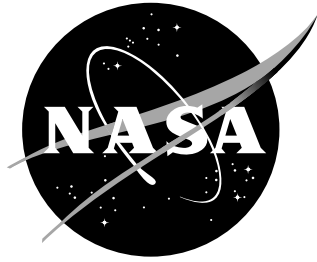


NASA/CR-2001-211056



Computational Analyses of Propulsion Aeroacoustics for Mixed Flow Nozzle Pylon Installation at Takeoff

*Steven J. Massey
Eagle Aeronautics, Inc., Hampton, Virginia*

*Kenrick A. Waithe
Analytical Services & Materials, Inc., Hampton, Virginia*

September 2001

The NASA STI Program Office ... in Profile

Since its founding, NASA has been dedicated to the advancement of aeronautics and space science. The NASA Scientific and Technical Information (STI) Program Office plays a key part in helping NASA maintain this important role.

The NASA STI Program Office is operated by Langley Research Center, the lead center for NASA's scientific and technical information. The NASA STI Program Office provides access to the NASA STI Database, the largest collection of aeronautical and space science STI in the world. The Program Office is also NASA's institutional mechanism for disseminating the results of its research and development activities. These results are published by NASA in the NASA STI Report Series, which includes the following report types:

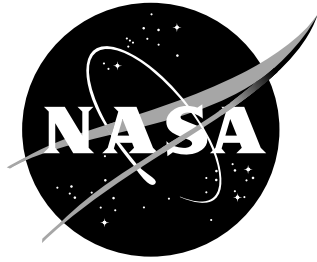
- TECHNICAL PUBLICATION. Reports of completed research or a major significant phase of research that present the results of NASA programs and include extensive data or theoretical analysis. Includes compilations of significant scientific and technical data and information deemed to be of continuing reference value. NASA counterpart of peer-reviewed formal professional papers, but having less stringent limitations on manuscript length and extent of graphic presentations.
- TECHNICAL MEMORANDUM. Scientific and technical findings that are preliminary or of specialized interest, e.g., quick release reports, working papers, and bibliographies that contain minimal annotation. Does not contain extensive analysis.
- CONTRACTOR REPORT. Scientific and technical findings by NASA-sponsored contractors and grantees.
- CONFERENCE PUBLICATION. Collected papers from scientific and technical conferences, symposia, seminars, or other meetings sponsored or co-sponsored by NASA.
- SPECIAL PUBLICATION. Scientific, technical, or historical information from NASA programs, projects, and missions, often concerned with subjects having substantial public interest.
- TECHNICAL TRANSLATION. English-language translations of foreign scientific and technical material pertinent to NASA's mission.

Specialized services that complement the STI Program Office's diverse offerings include creating custom thesauri, building customized databases, organizing and publishing research results ... even providing videos.

For more information about the NASA STI Program Office, see the following:

- Access the NASA STI Program Home Page at <http://www.sti.nasa.gov>
- E-mail your question via the Internet to help@sti.nasa.gov
- Fax your question to the NASA STI Help Desk at (301) 621-0134
- Phone the NASA STI Help Desk at (301) 621-0390
- Write to:
NASA STI Help Desk
NASA Center for AeroSpace Information
7121 Standard Drive
Hanover, MD 21076-1320

NASA/CR-2001-211056



Computational Analyses of Propulsion Aeroacoustics for Mixed Flow Nozzle Pylon Installation at Takeoff

*Steven J. Massey
Eagle Aeronautics, Inc., Hampton, Virginia*

*Kenrick A. Waithe
Analytical Services & Materials, Inc., Hampton, Virginia*

National Aeronautics and
Space Administration

Langley Research Center
Hampton, Virginia 23681-2199

Prepared for Langley Research Center
under Purchase Order L-13395

September 2001

Available from:

NASA Center for AeroSpace Information (CASI)
7121 Standard Drive
Hanover, MD 21076-1320
(301) 621-0390

National Technical Information Service (NTIS)
5285 Port Royal Road
Springfield, VA 22161-2171
(703) 605-6000

Computational Analyses of Propulsion Aeroacoustics for Mixed Flow Nozzle Pylon Installation at Takeoff

Steven J. Massey
Eagle Aeronautics, Inc.
Hampton, VA

Kenrick A. Waithe
Analytical Services and Materials, Inc.
Hampton, VA

June 21, 2001

1 Introduction

The objective of this task is to perform CFD analyses of a set of baseline and noise suppression mixed flow nozzles with and without a pylon installation. This paper presents the full CFD results from which the principal investigators of the study have recently published a conference paper, Thomas *et al.* [1]. The five model configurations are as follows; a baseline core/fan dual-stream nozzle with an external plug, a chevron mixer nozzle with a peak on the symmetry plane with external plug, both of the above nozzles with an installed bifurcating pylon and lastly a clocked chevron mixer nozzle such that a trough is aligned with the center of the pylon. All grids cover 180° of the nozzle. The grids were constructed by GeoLab at LaRC under a separate task. Since the cases were solved using two schemes, time marching for the nozzle region and space marching for the far-field plume, the cell counts for the two regions for each case are given separately in Table 1. In this study the flight takeoff (TKO) flow conditions are solved on all models, see Table 2.

Table 1: Grid Size in Cells

Case	Geometry	Time Marched	Space Marched	Total
		Nozzle	Plume	
1	Round Nozzle	4,083,072	1,797,120	5,880,192
2	Round Nozzle w/ Pylon	7,805,440	3,594,240	11,399,680
3	Chevron Nozzle	10,125,312	3,594,240	13,719,552
4	Chevron Tip under Pylon	12,620,096	3,594,240	16,214,336
5	Chevron Trough under Pylon	13,383,744	3,594,240	16,977,984

Table 2: Flow condition definitions.

Flow Condition	Mach	P_t [psi]	T_t [R]	FPR	CPR	Fan T_t [R]	Core T_t [R]
Takeoff (TKO)	0.28	14.7	530.	1.75	1.56	647.	1491.

2 Numerical Method

The fluid flow is simulated by solving the asymptotically steady, compressible, Reynolds-averaged Navier-Stokes equations using an implicit, up-wind, flux-difference splitting finite volume scheme and standard two equation $k-\varepsilon$ turbulence model with a linear stress representation. All computations are performed using the multiblock, parallel, structured code PAB3D [2]. Solutions are obtained using the flux difference splitting scheme of Roe, uncoupled viscosity in the normal and circumferential directions, linear $k-\varepsilon$ turbulence model, and a 2-factor scheme for the approximation of implicit terms. Grid sequencing is used to accelerate convergence by solving 1/4 then 1/2 of the grid in each of the three computational directions. The general solution procedure followed is to solve the region near the nozzle via time marching, then solve the plume blocks via space marching, then finally run a comparatively small number of time marching iterations on the plume blocks and adjacent upstream blocks in order to smooth any inflections at the time/space marching block boundary. Wall clock run-time using four Compaq Alpha 500 MHz machines in parallel is (depending on grid size) approximately 50 to 150 hours for time marching of the nozzle and nearby plume, 3-6 hours to space march the plume, and 4-8 hours to smooth out the solution by time marching the plume. The final plume time marching is optional since the space marched solution is already well converged. Due to the large size of these cases, they will scale very efficiently to the larger clusters as they become available.

3 Results

In this study, the effects of geometry changes are sought on the precursors of noise, such as turbulence and vorticity. It is hoped that any geometry change will not have a significant effect on the performance of the nozzle. Grids and flooded solution contours are presented in Figures 1-34 for the five cases identified in Table 1. Pylon flow topology is shown in Figures 35 and 36. Model comparisons for axial variation of mass averaged quantities with integration lower limits set to 100.5% of freestream T_t and 100.5% of fan T_t are plotted in Figures 37 and 38 respectively. Mass averaged quantities are calculated at each axial station by integrating over the area that contains flow above the chosen total temperature, for example,

$$k_{ave} = \frac{\int_A k \rho u \, dA}{\int_A \rho u \, dA} \quad (1)$$

with integration only performed over areas where

$$T_t \geq 1.005T_{t\infty} \text{ or } T_{t_{FAN}}. \quad (2)$$

Non-dimensional forms of total temperature and turbulence kinetic energy are shown in Figures 39 and 40 respectively. The non-dimensional expressions are identical to those

published by Kenzakowski *et al.* [3] and are defined as follows:

$$\text{Non-dimensional Average Total Temperature} = \frac{\int_A \phi \rho u \, dA}{\int_A \rho u \, dA} \quad (3)$$

$$\text{Average Turbulence Intensity} = \frac{\int_A \sqrt{\frac{k}{q}} \rho u \, dA}{\int_A \rho u \, dA} \quad (4)$$

where

$$\phi = \frac{T_t - T_{t_{FAN}}}{T_{t_{CORE}} - T_{t_{FAN}}} \quad (5)$$

with integration only performed over areas where

$$0.005 \leq \phi \leq 1. \quad (6)$$

The integrations were implemented using a combination of Tecplot scripts and Fortran code written by the authors specifically for this task. Lastly, axial variation of maximum total temperature and specific turbulence kinetic energy are plotted in Figures 41 and 42 respectively.

3.1 Case 1, Round Nozzle

The round nozzle case is the baseline case from which the effects of the pylon and chevrons will be evaluated. Although the geometry is axisymmetric, the case is still run as a 3-D half plane with the same grid topology as the other cases, Figure 1. A typical maximum flow vector residual history is shown in Figure 2, where the spikes highlight the change in grid sequencing from 444 to 222 to 111. Because the round case is coarser than the other cases, residual dropped only by a little more than three orders of magnitude. Finer cases typically drop by more than four.

Contours of Mach number, P_t and T_t , shown in Figures 3-5, depict a clean symmetric solution, despite the many block boundaries and the fact that the solution was space marched beyond $x = 13.7$ core diameters. Note, in all cases length is in terms of the round nozzle core diameter with the origin at the fan exit. For all T_t plots the contours are cutoff below 100.5% of freestream. Vertical cross-flow planes at $x = 2, 4, 8, 16$ core diameters, Figures 6 and 7, indicate a well developed solution with no asymmetry except for the log vorticity magnitude. $\ln \omega$ is very sensitive to any solution fluctuations as well as grid quality.

3.2 Case 2, Round Nozzle w/ Pylon

Figure 8 depicts the pylon and nozzle grid surfaces in black against the blue symmetry plane. Close-up rotated views of the pylon/nozzle interface are shown in Figure 9. Symmetry plane plots, Figures 10-12, show the strong vertical influence of the pylon (and lower bifurcator) on the jet flow. Cross-flow plots, Figures 13-14, clarify the effect by showing the location of the pylon in the flow and its azimuthal influence. It is clear from the pressure and total temperature plots, that the pylon shields the top portion of the core flow from the high pressure fan flow. This allows the core flow to follow the bottom contour of the pylon, which

due to its upward curvature imparts significant upward momentum. In comparison to the baseline round case, a large increase of k can be seen in the $x = 8$ plane. As noise is a function of turbulence, this peak is a likely source for noise.

3.3 Case 3, Chevron Nozzle

Symmetry plane views show a well developed and vertically symmetric solution for the chevron case, Figures 16-18. Because of the star-like cross-flow pattern caused by the chevrons, contours on the symmetry plane can be misleading. An example of this is the apparent source of T_t near the $x = 6$ station, which is simply the cross-flow lobe moving closer to the symmetry plane. Cross-flow images, Figures 19-20 are all very symmetric and indicate that future studies without a pylon may be carried out on 1/8 sector rather than the present 1/2. The chevrons mix the flow very well while at the same time reducing average and peak specific turbulence kinetic energy levels, Figures 37 and 42.

3.4 Case 4, Chevron Tip under Pylon

In this case, the pylon was added to the chevron geometry, Figure 21. Close-up rotated views of the pylon/chevron interface are shown in Figure 22. The introduction of the pylon to the chevron jet flow produces the same effect as on the round jet, Figures 23-25. The new feature is the top lobe of core flow is now drawn into the pylon, Figures 26-27, which produces a strong attachment line coupled with a spiral separation on each side of the bottom the pylon, Figure 35.

3.5 Case 5, Chevron Trough under Pylon

The final case is constructed by rotating the chevrons such that the trough lies directly under the center of the pylon, Figures 28-29. Moving the trough under the pylon has the very beneficial effect of splitting a single cross-flow plume on the pylon, Figure 33, which reduces the energy available to the pylon boundary layer and fan shear layer and thus results in much lower specific turbulence kinetic energy levels, Figure 34. Separation is also reduced and moved to the sharp outer edge of the pylon, Figure 36. A strong attachment line is also observed in close alignment with the chevron edge on the bottom of the pylon. For reference, the round nozzle with pylon case did not incur any flow separation on the pylon and both chevron with pylon cases did not have any further flow topology features outside the boundaries of the figures shown, Figures 35 and 36.

3.6 Axial Distributions

With the exception of turbulence kinetic energy and vorticity, mass averaged quantities of the full jet using a temperature integration lower limit of 100.5% of T_{t_∞} are largely diluted by the inclusion of fan flow, Figure 37. To better isolate the mixing between the fan and core flows, averages are taken using a temperature integration lower limit of 100.5% of $T_{t_{FAN}}$, Figure 38. From the latter set of averages, and the non-dimensional averages, Figures 39 and 40, it is clear that the core chevrons significantly enhance mixing while the pylon itself

provides a slight increase in mixing for round and chevron cases. In terms of peak turbulence kinetic energy, Figure 42, the clocked chevron is much lower than the other pylon cases, while slightly higher than the no-ylon cases.

4 Concluding Remarks

In general the cases ran very well. Techniques have been developed to extract quantitative characterizations of the jet flows. Further study is required to refine expressions which are indicative of noise and mate these with rigorous noise prediction models. It is concluded that the clocked chevron with pylon case achieves the most optimal levels of average and peak turbulence kinetic energy and vorticity and therefore is expected to be the quietest of the five configurations tested.

The authors wish to gratefully acknowledge the Configuration Aerodynamics Branch of LaRC for the use of their Alpha clusters to complete the cases in this study. All data and post processing files and scripts are included in the deliverables on CD-ROM.

References

- [1] Thomas, R. H., Kinzie, K. W., and Pao, S. P., "Computational Analysis of a Pylon-Chevron Core Nozzle Interaction," AIAA Paper 2001-2185, 2001.
- [2] Abdol-Hamid, K. S., "Development of Three-Dimensional Code for the Analysis of Jet Mixing Problem," NASA CR 4200, 1988.
- [3] Kenzakowski, D. C., Shipman, J., and Dash, S. M., "Turbulence Model Study of Laboratory Jets with Mixing Enhancements for Noise Reduction," AIAA Paper 2000-0219, 2000.

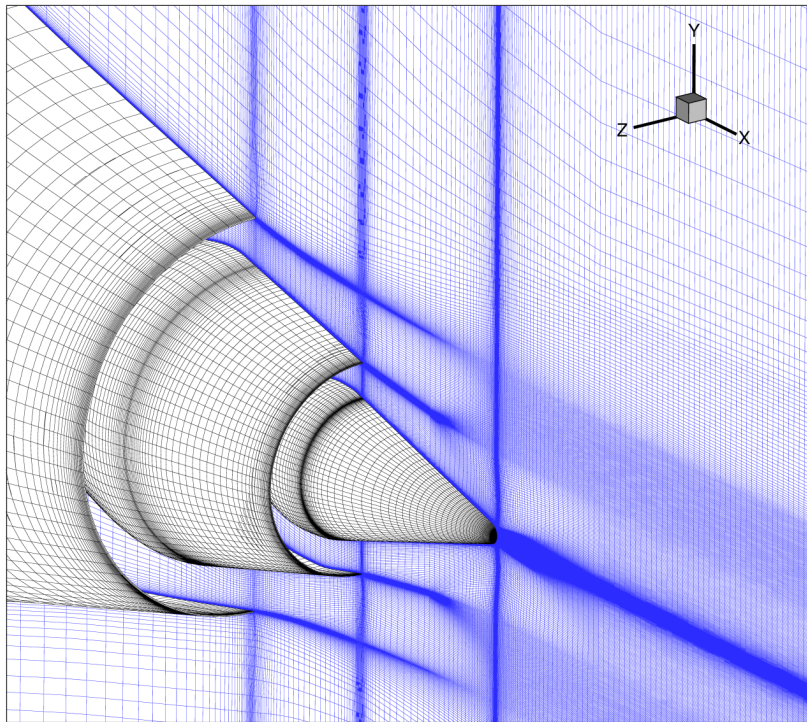


Figure 1: Case 1, Round Nozzle: grid close-up view, with symmetry plane shown in blue.

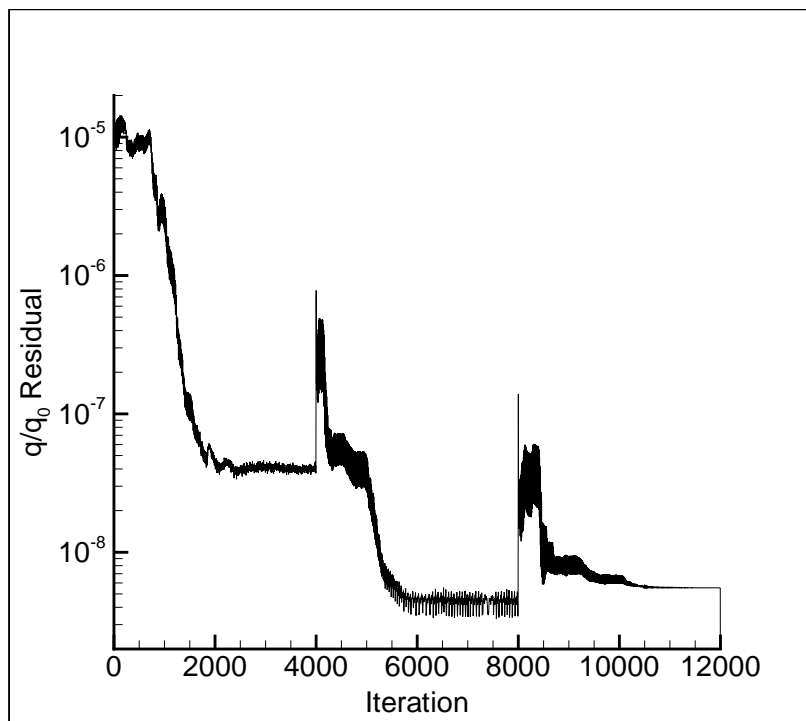


Figure 2: Case 1, Round Nozzle: residual history.

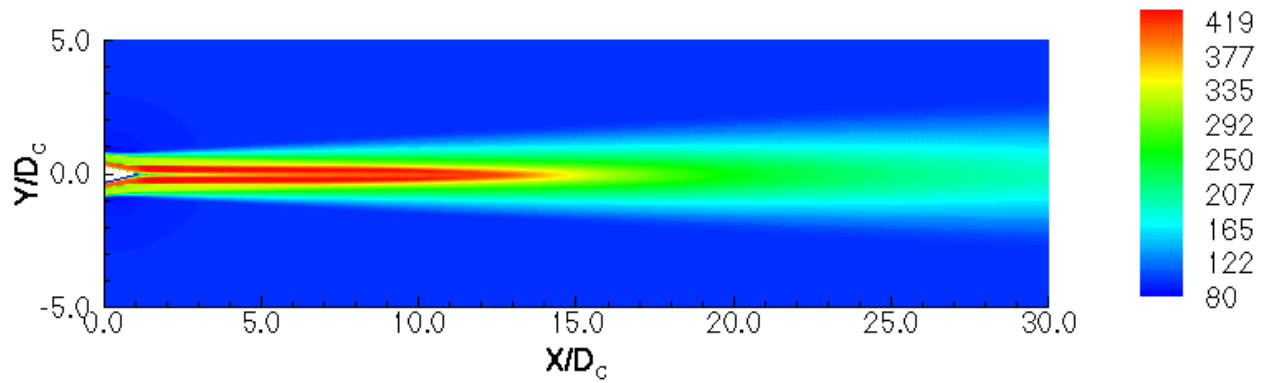


Figure 3: Case 1, Round Nozzle: Axial Velocity [m/s] contours.

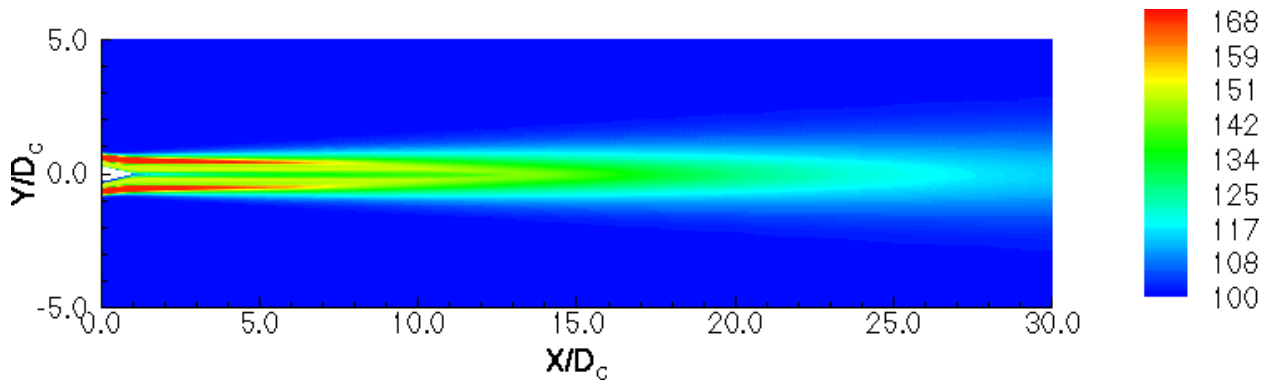


Figure 4: Case 1, Round Nozzle: Total Pressure [kPa] contours.

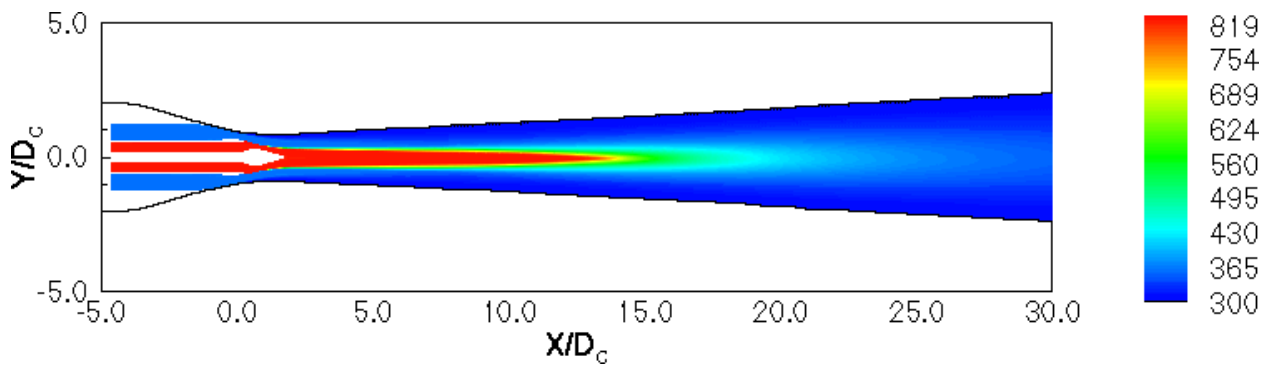


Figure 5: Case 1, Round Nozzle: Total Temperature [K] contours.

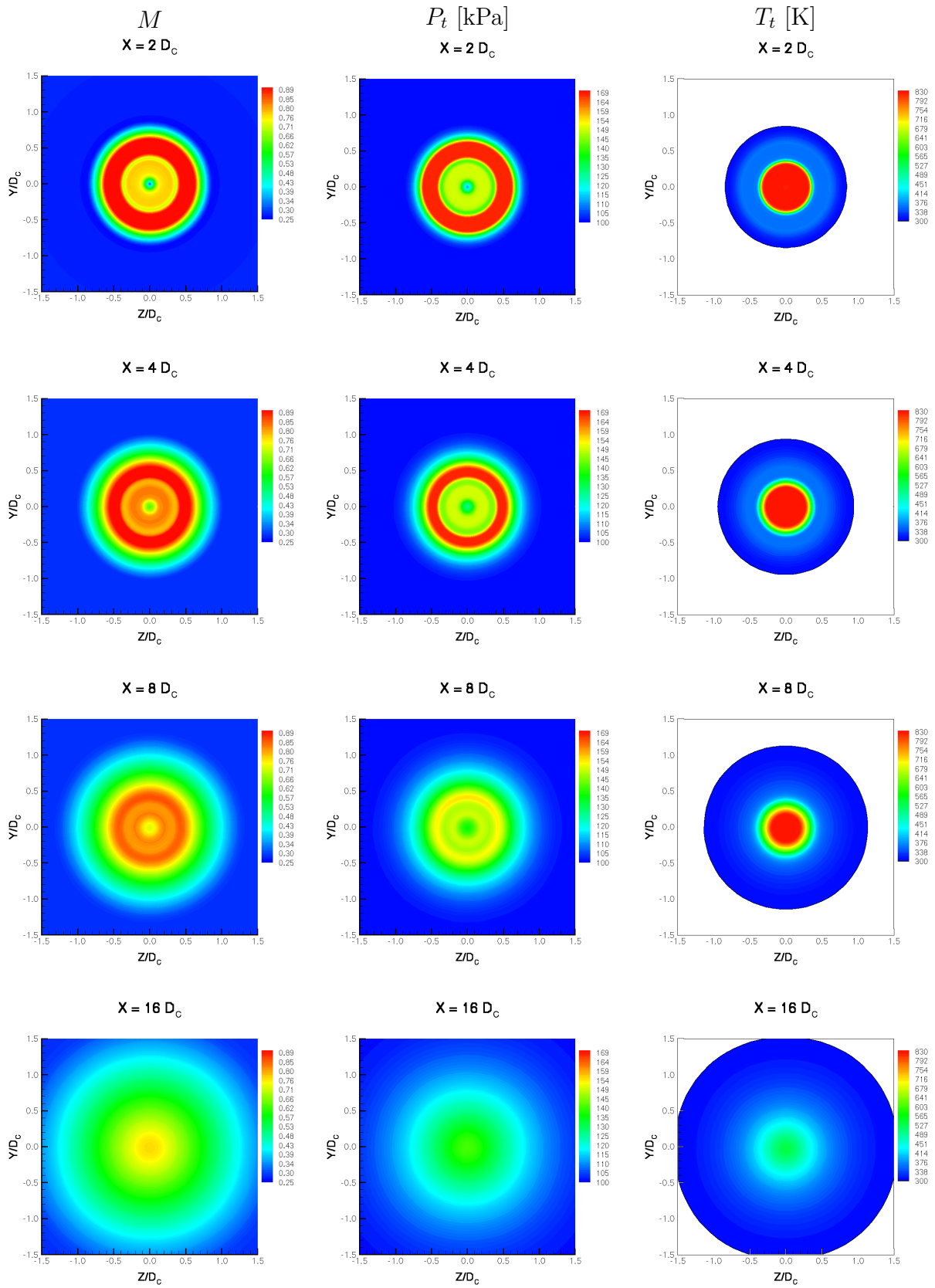


Figure 6: Case 1, Round Nozzle: Mach number, Total Pressure[kPa] and Total Temperature [K] contours at stream-wise stations $x = 2, 4, 8, 16$ core diameters, starting from the fan exit.

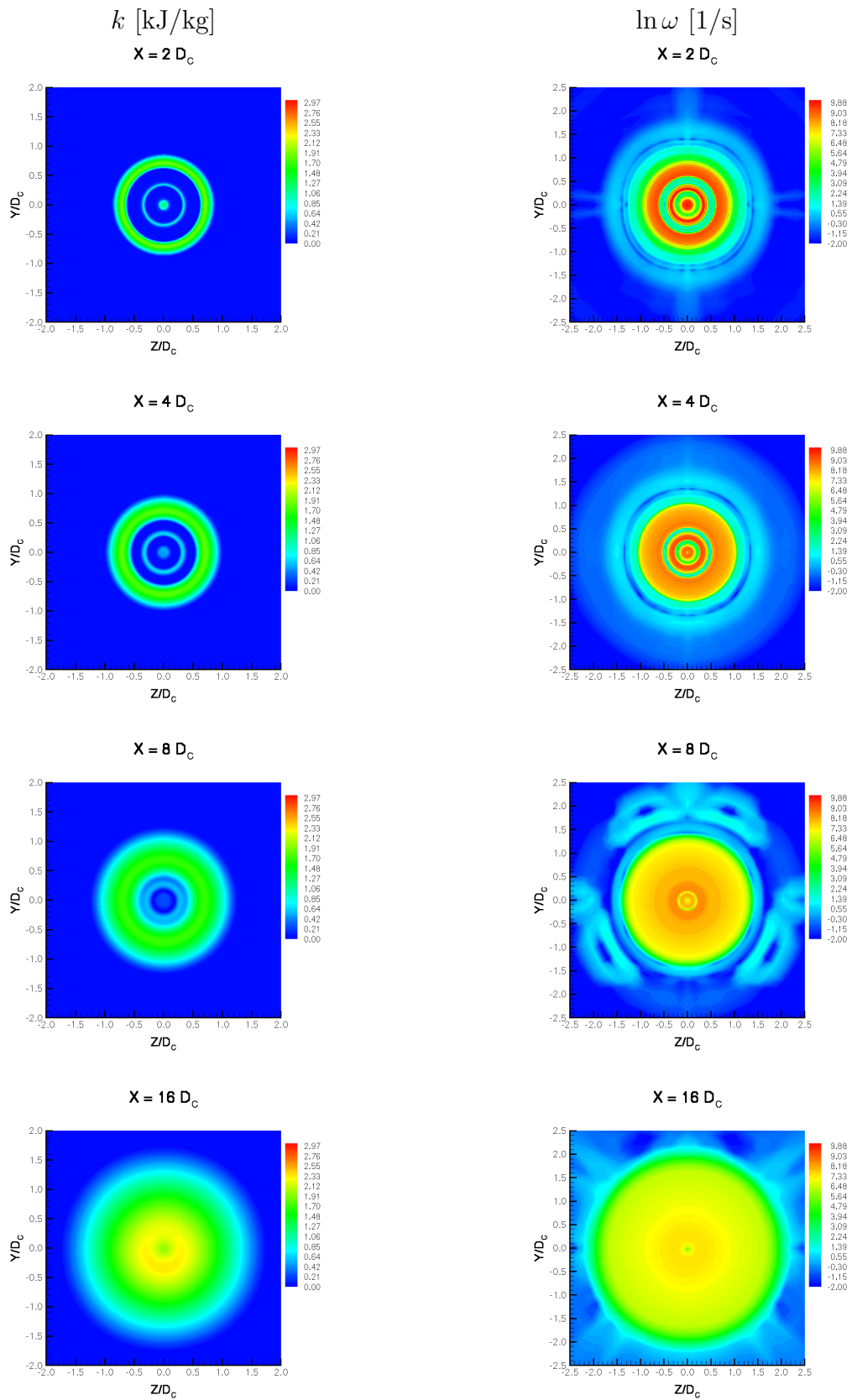


Figure 7: Case 1, Round Nozzle: Specific Turbulence Kinetic Energy [kJ/kg] and Log Vorticity Magnitude [1/s] contours at stream-wise stations $x = 2, 4, 8, 16$ core diameters, starting from the fan exit.

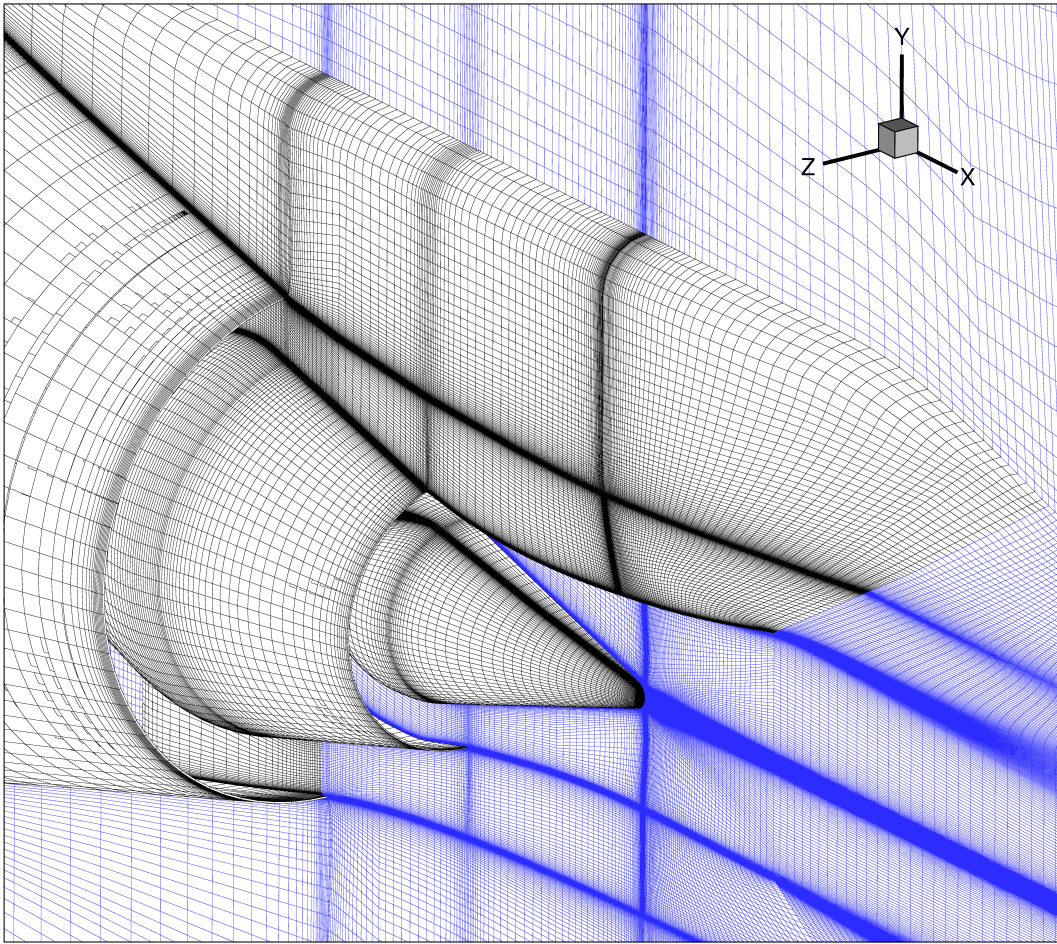


Figure 8: Case 2, Round Nozzle w/ Pylon: grid close-up view, with symmetry plane shown in blue.

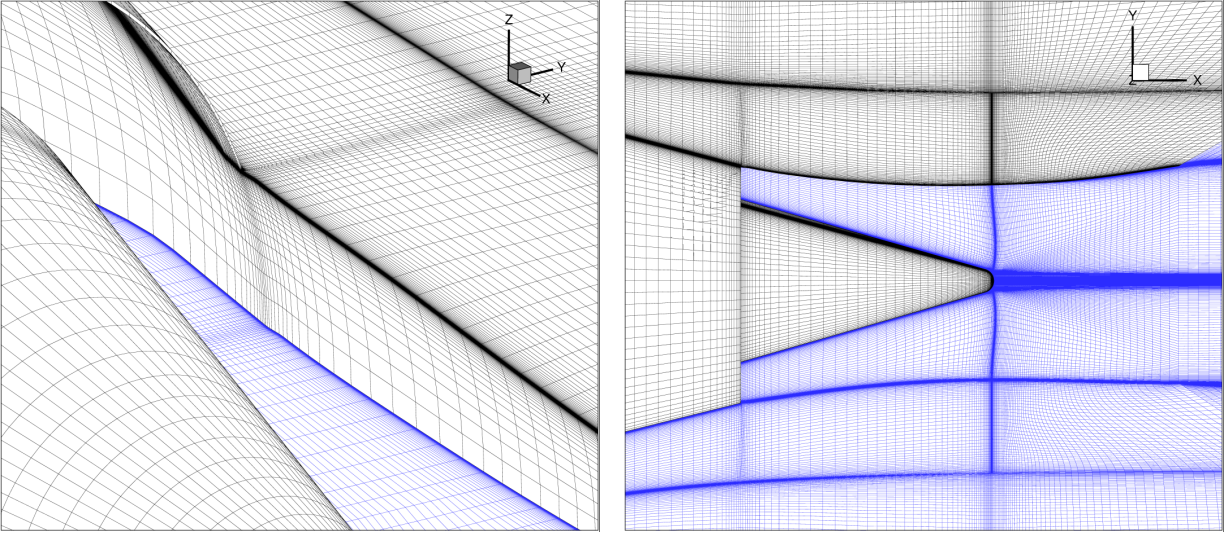


Figure 9: Case 2, Round Nozzle w/ Pylon: pylon grid interface views, with symmetry plane shown in blue.

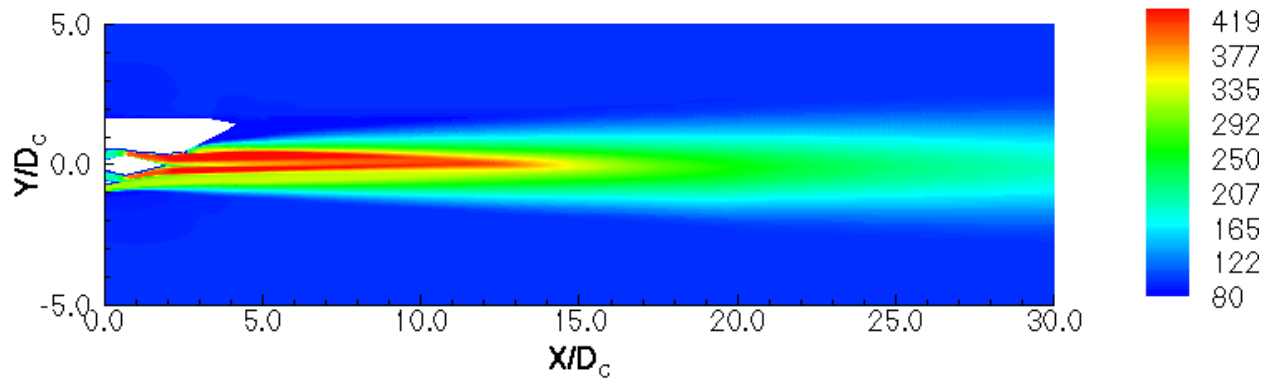


Figure 10: Case 2, Round Nozzle w/ Pylon Axial Velocity [m/s] contours.

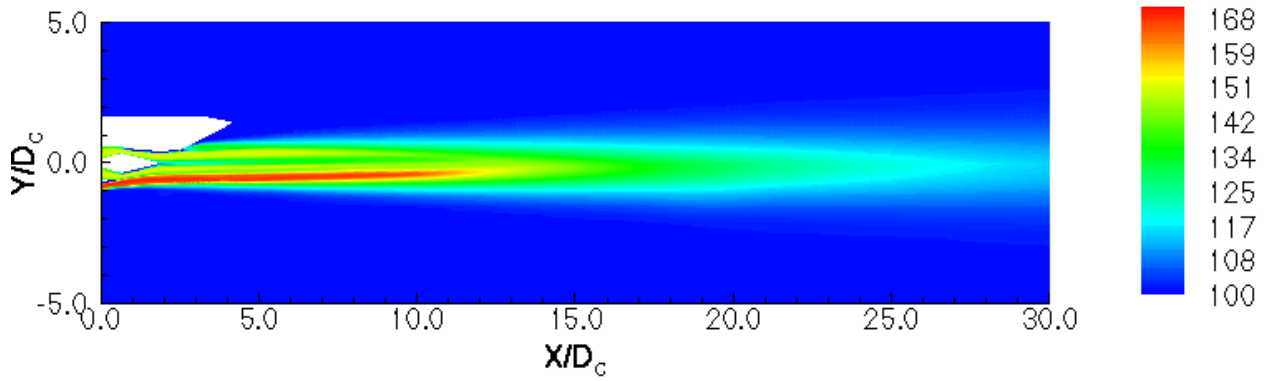


Figure 11: Case 2, Round Nozzle w/ Pylon: Total Pressure [kPa] contours.

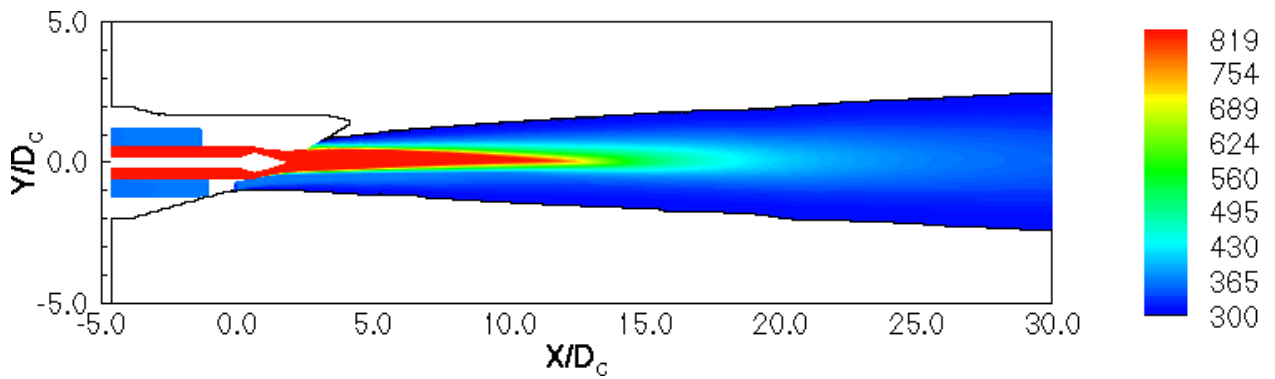


Figure 12: Case 2, Round Nozzle w/ Pylon: Total Temperature [K] contours.

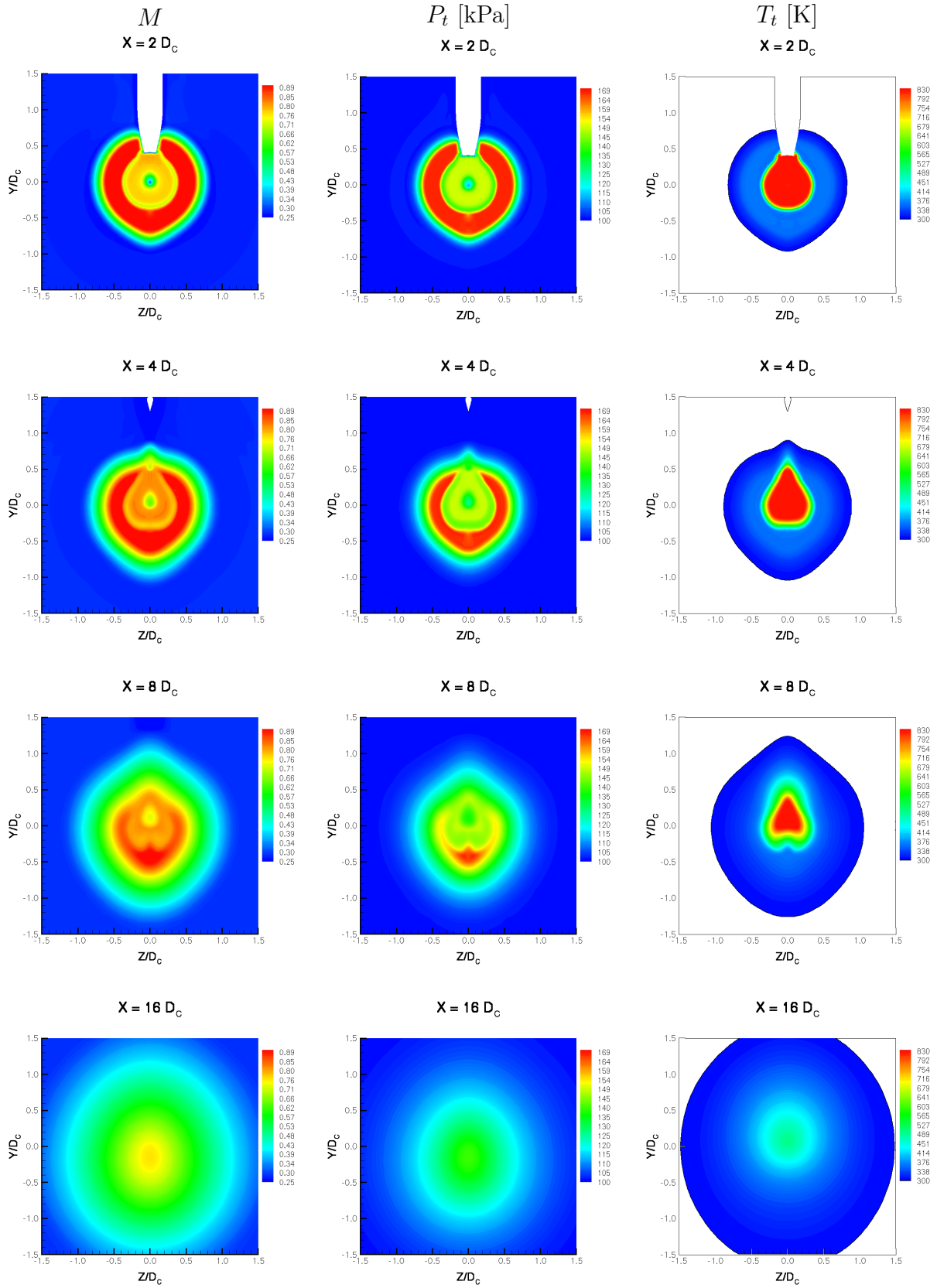


Figure 13: Case 2, Round Nozzle w/ Pylon: Mach number, Total Pressure[kPa] and Total Temperature [K] contours at stream-wise stations $x = 2, 4, 8, 16$ core diameters, starting from the fan exit.

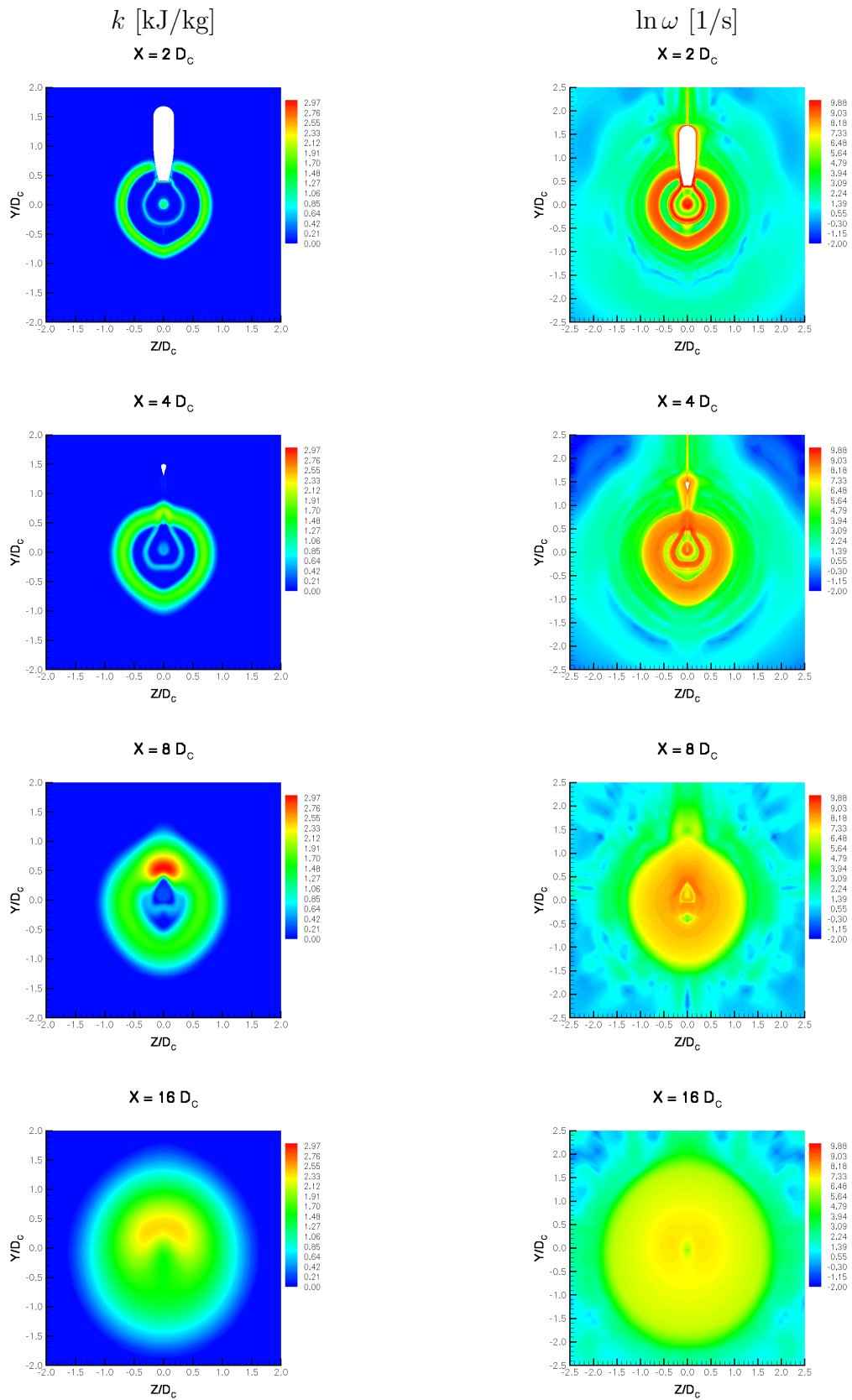


Figure 14: Case 2, Round Nozzle w/ Pylon: Specific Turbulence Kinetic Energy [kJ/kg] and Log Vorticity Magnitude [1/s] contours at stream-wise stations $x = 2, 4, 8, 16$ core diameters, starting from the fan exit.

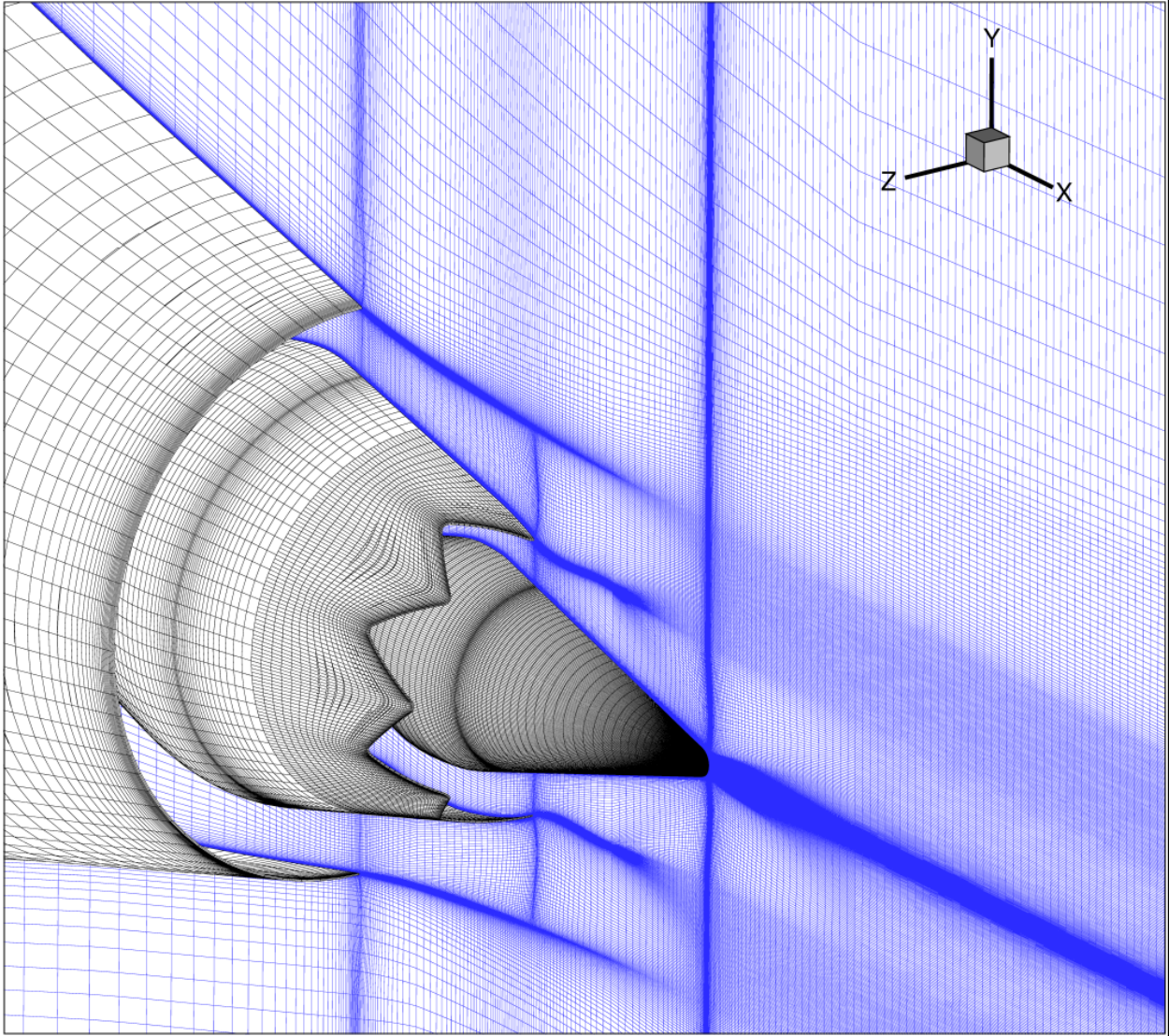


Figure 15: Case 3, Chevron Nozzle: grid close-up view, with symmetry plane shown in blue.

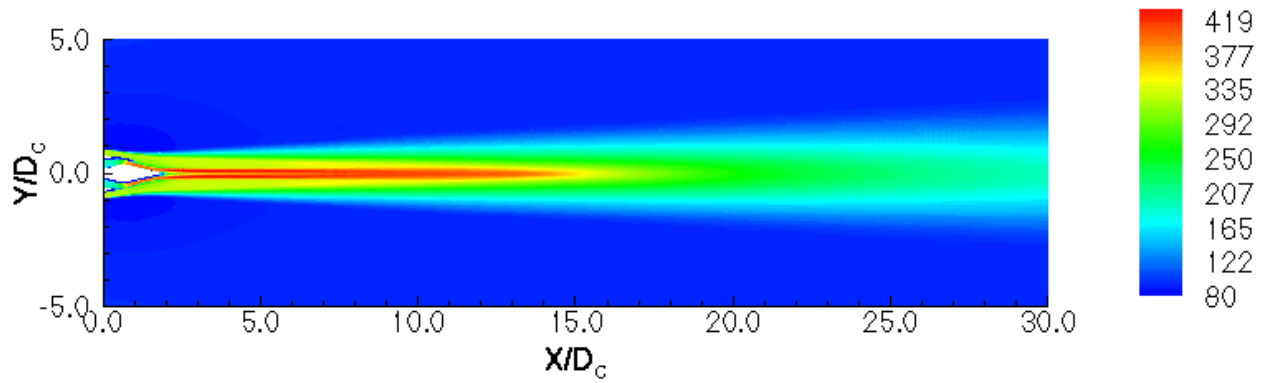


Figure 16: Case 3, Chevron Nozzle Axial Velocity [m/s] contours.

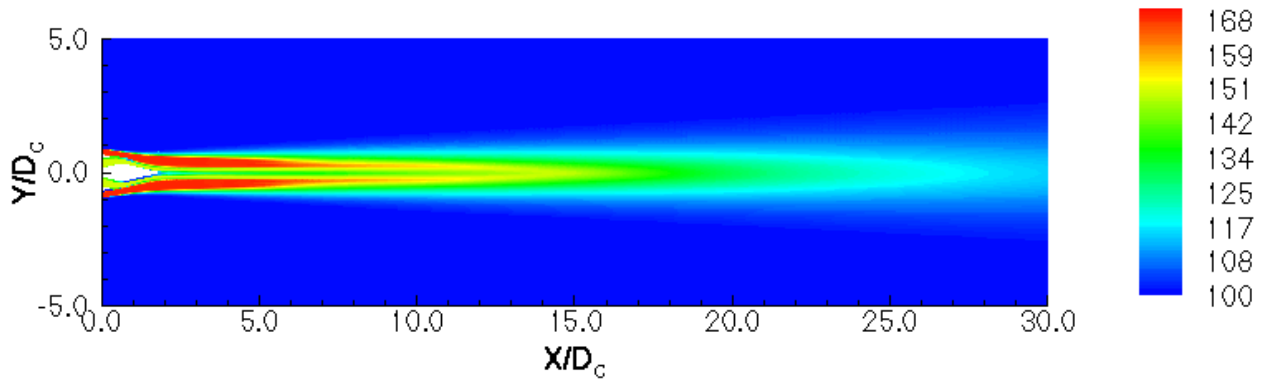


Figure 17: Case 3, Chevron Nozzle: Total Pressure [kPa] contours.

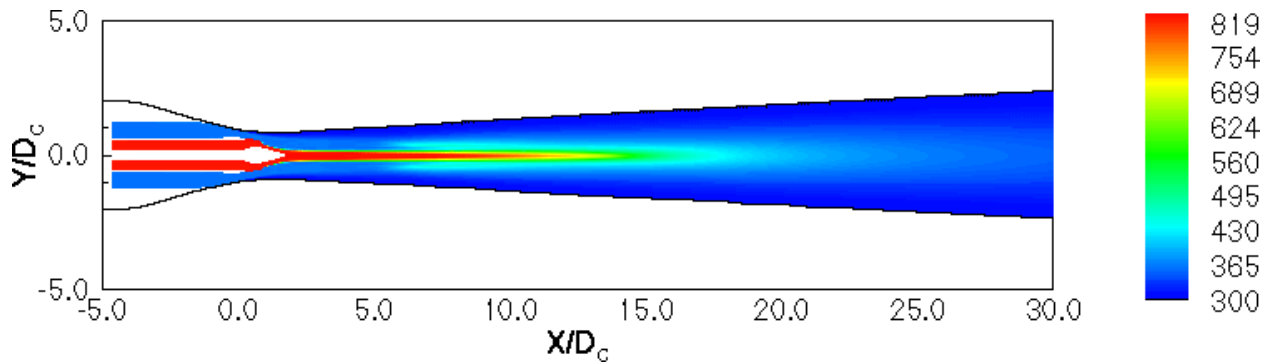


Figure 18: Case 3, Chevron Nozzle: Total Temperature [K] contours.

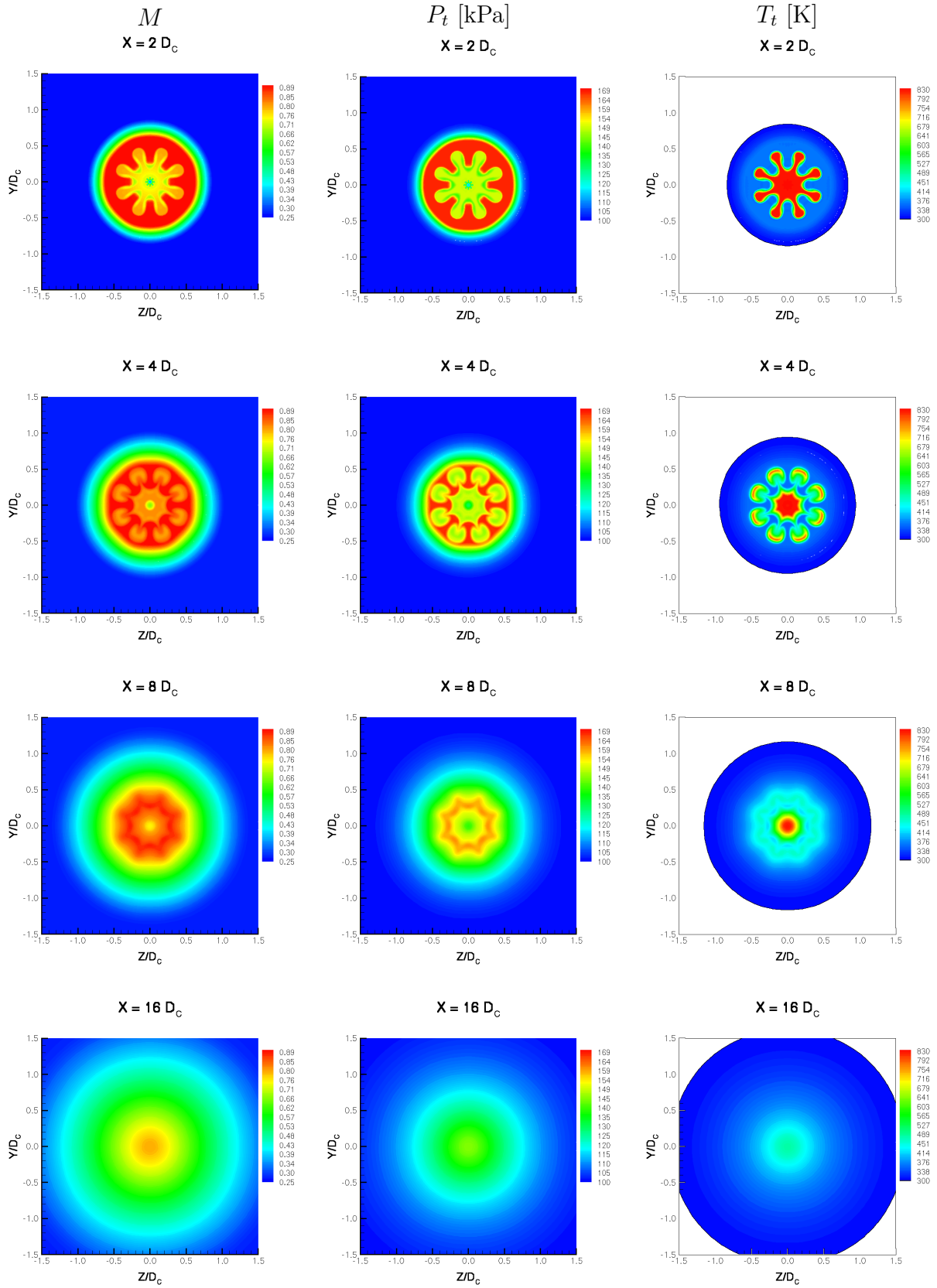


Figure 19: Case 3, Chevron Nozzle: Mach number, Total Pressure[kPa] and Total Temperature [K] contours at stream-wise stations $x = 2, 4, 8, 16$ core diameters, starting from the fan exit.

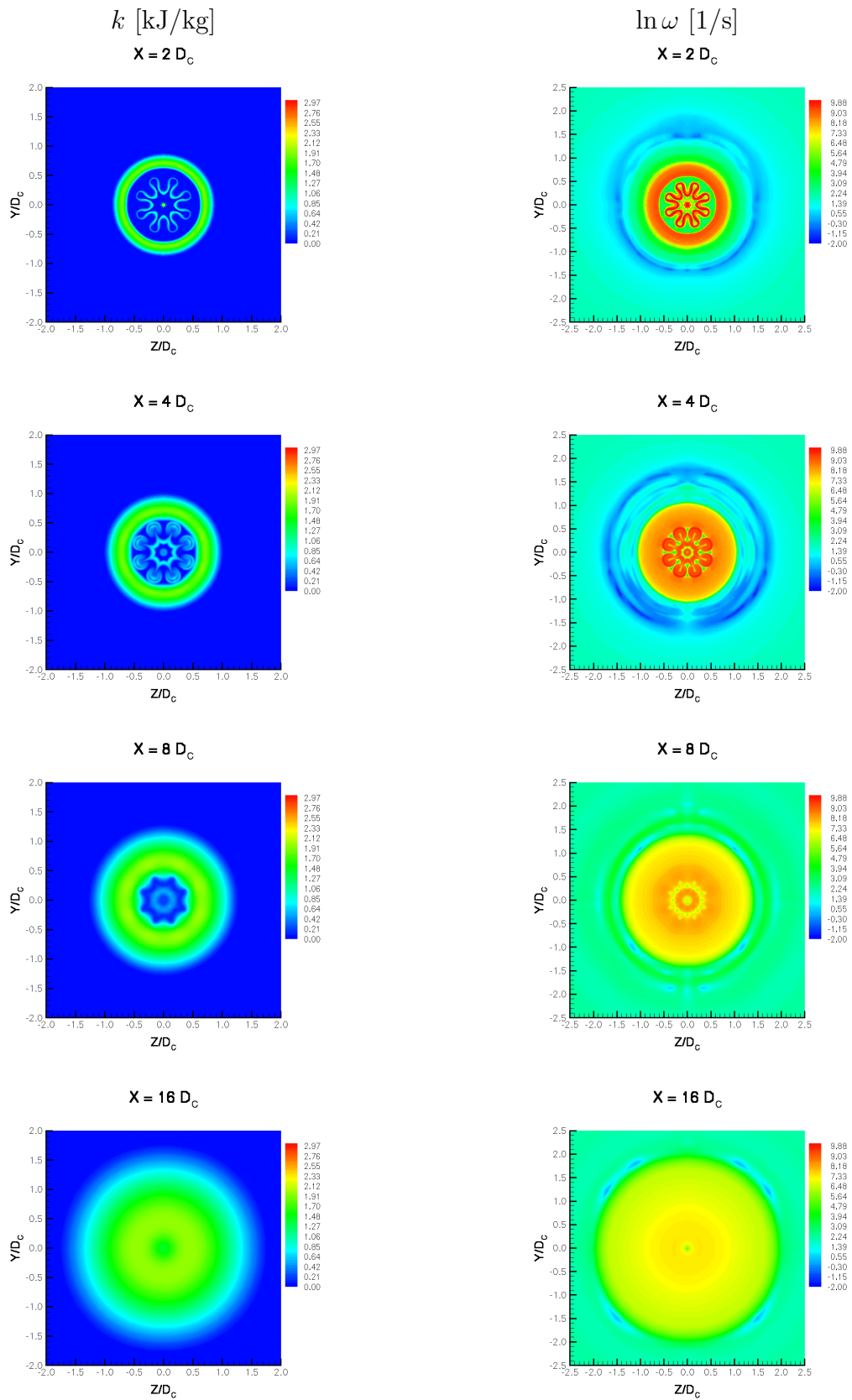


Figure 20: Case 3, Chevron Nozzle: Specific Turbulence Kinetic Energy [kJ/kg] and Log Vorticity Magnitude [1/s] contours at stream-wise stations $x = 2, 4, 8, 16$ core diameters, starting from the fan exit.

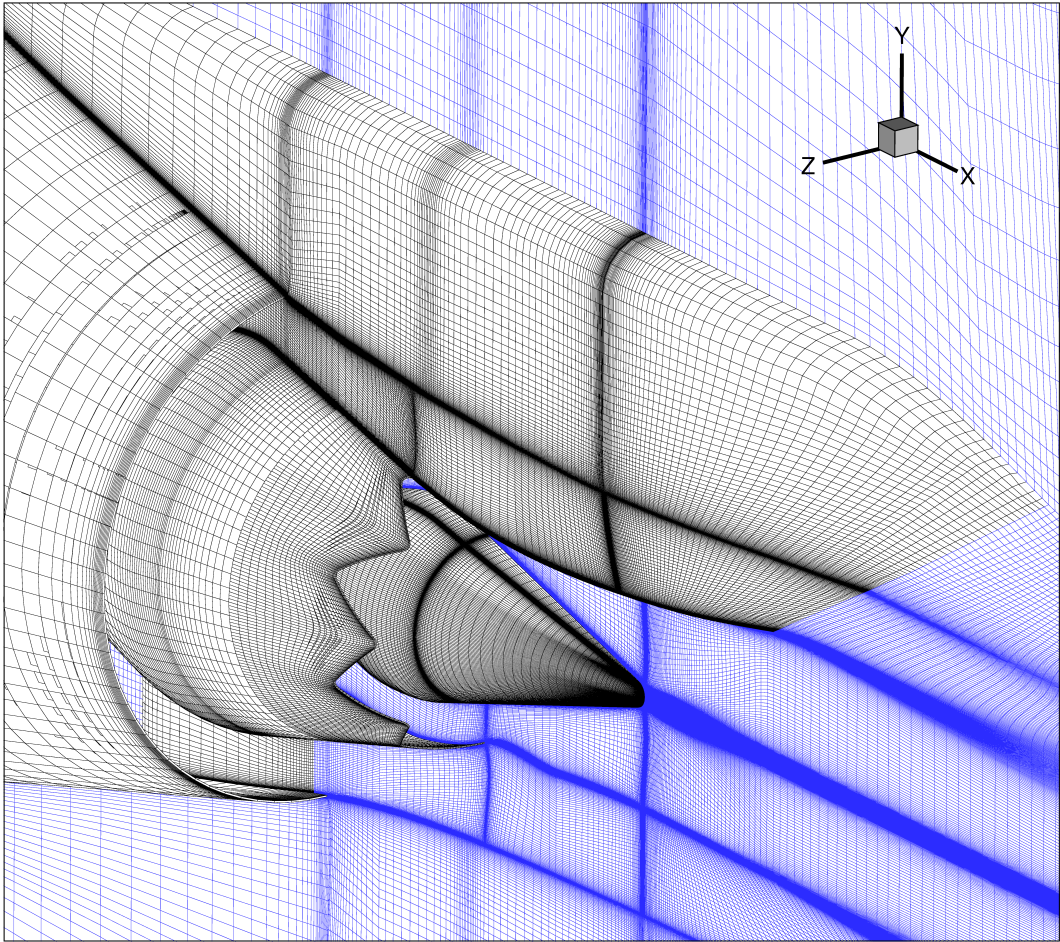


Figure 21: Case 4, Chevron Tip under Pylon: grid close-up view, with symmetry plane shown in blue.

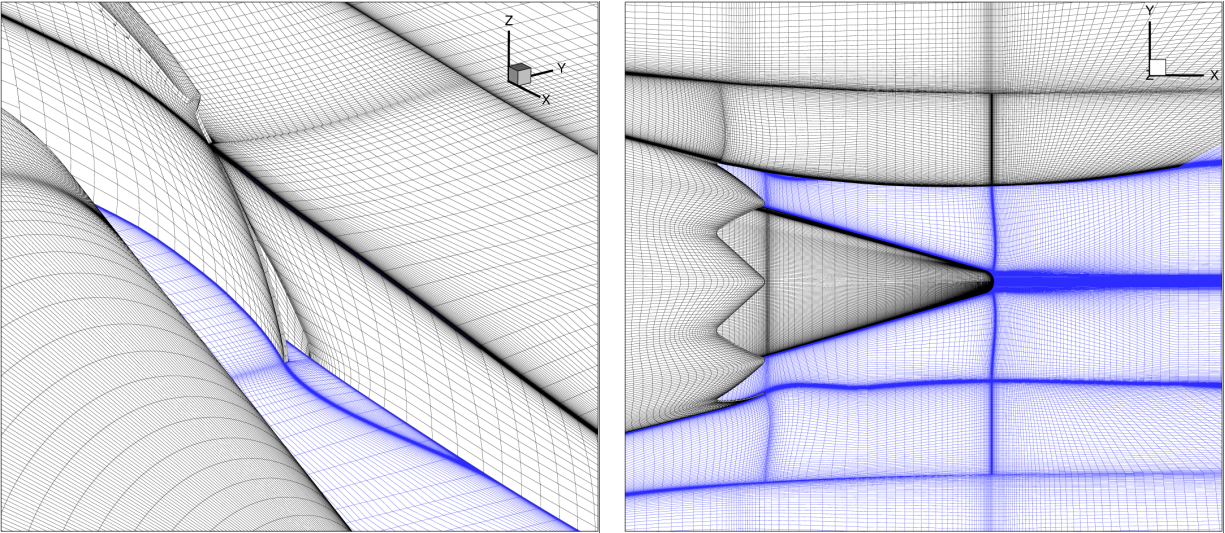


Figure 22: Case 4, Chevron Tip under Pylon: pylon grid interface views, with symmetry plane shown in blue.

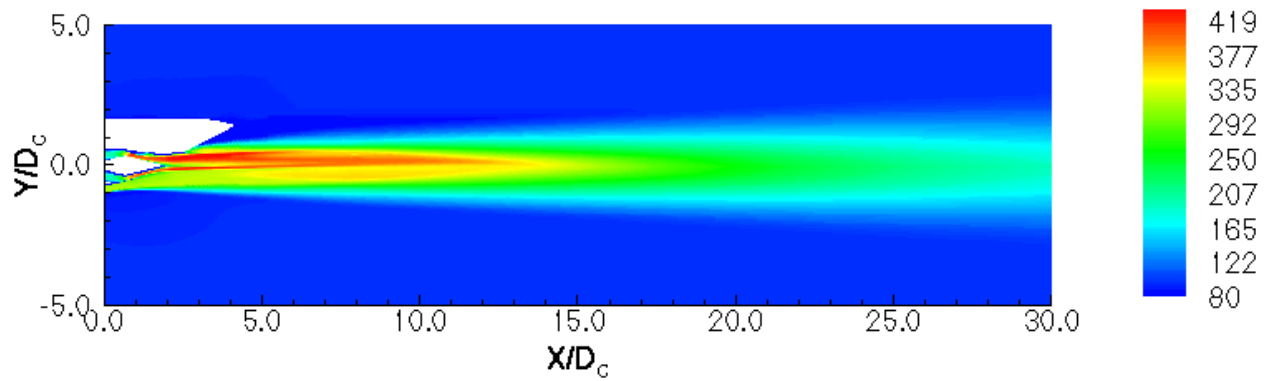


Figure 23: Case 4, Chevron Tip under Pylon Axial Velocity [m/s] contours.

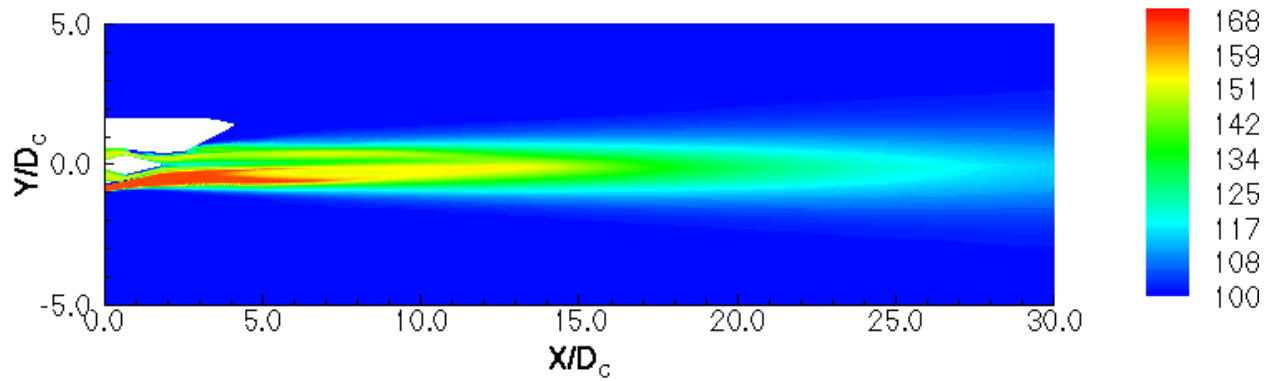


Figure 24: Case 4, Chevron Tip under Pylon: Total Pressure [kPa] contours.

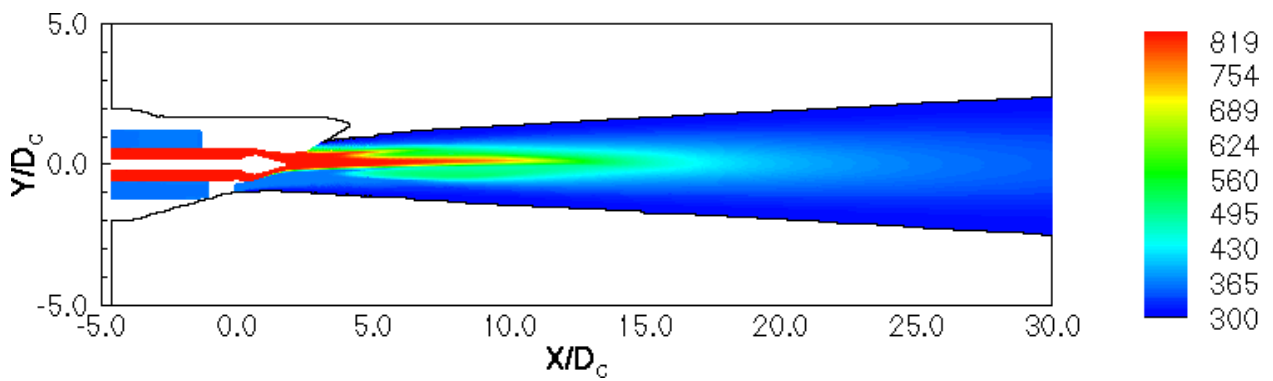


Figure 25: Case 4, Chevron Tip under Pylon: Total Temperature [K] contours.

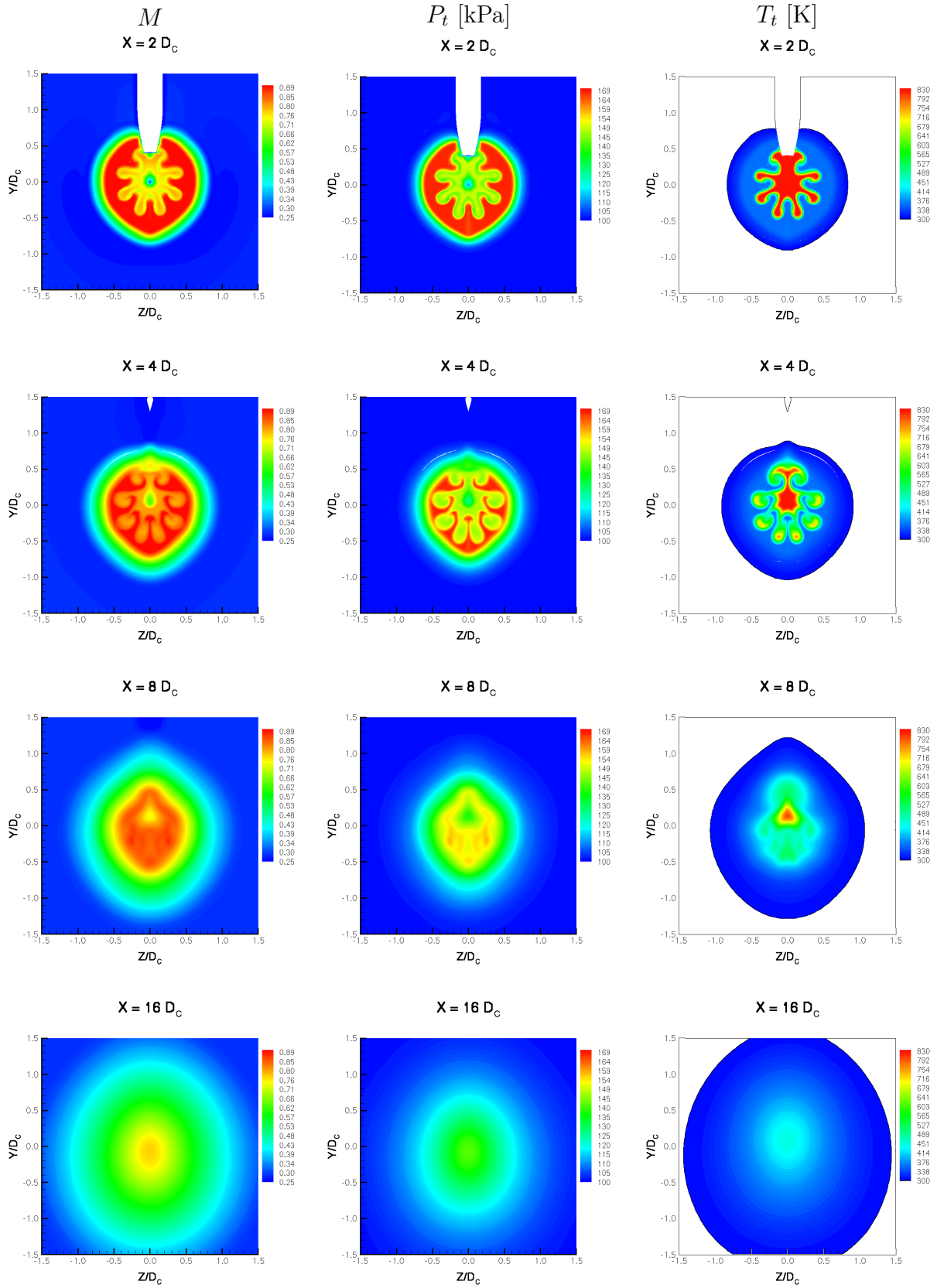


Figure 26: Case 4, Chevron Tip under Pylon: Mach number, Total Pressure[kPa] and Total Temperature [K] contours at stream-wise stations $x = 2, 4, 8, 16$ core diameters, starting from the fan exit.

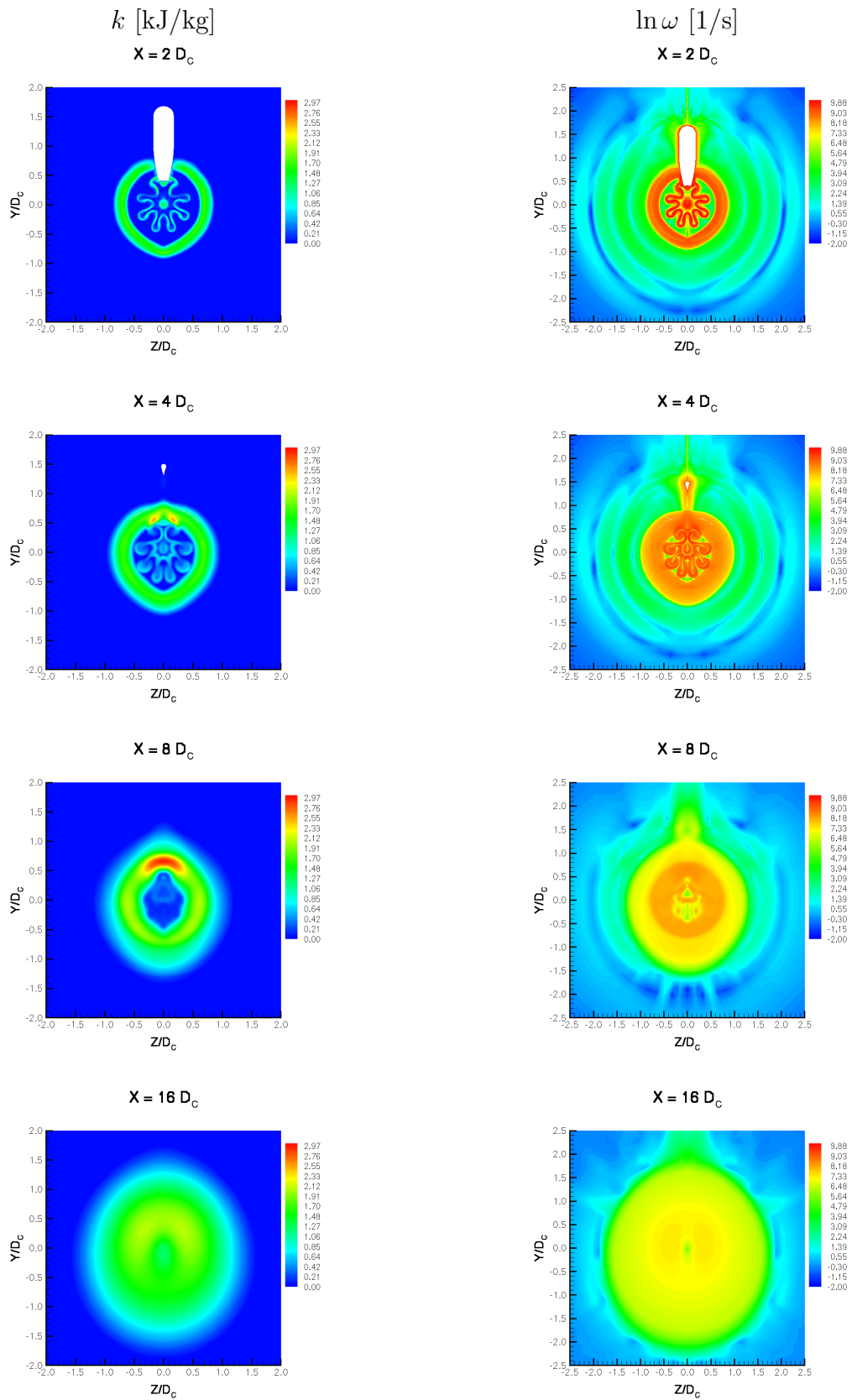


Figure 27: Case 4, Chevron Tip under Pylon: Specific Turbulence Kinetic Energy [kJ/kg] and Log Vorticity Magnitude [1/s] contours at stream-wise stations $x = 2, 4, 8, 16$ core diameters, starting from the fan exit.

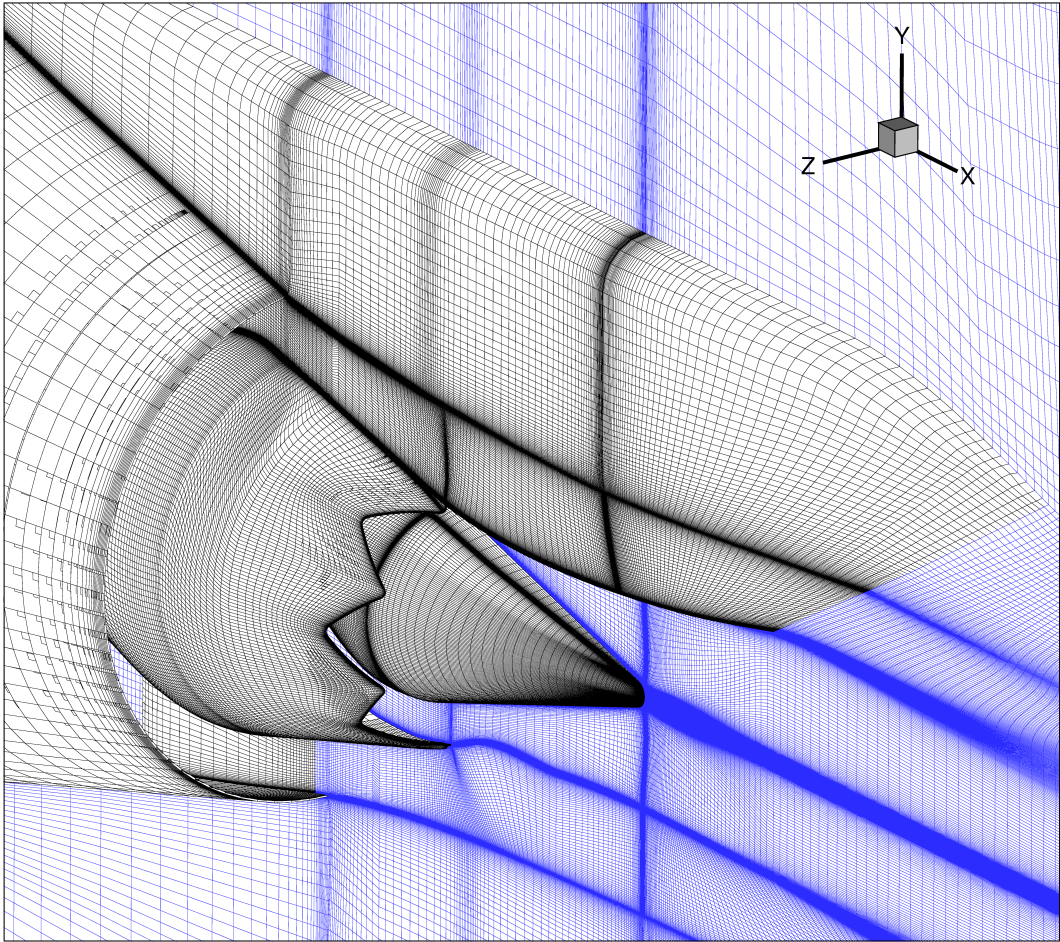


Figure 28: Case 5, Chevron Trough under Pylon: grid close-up view, with symmetry plane shown in blue.

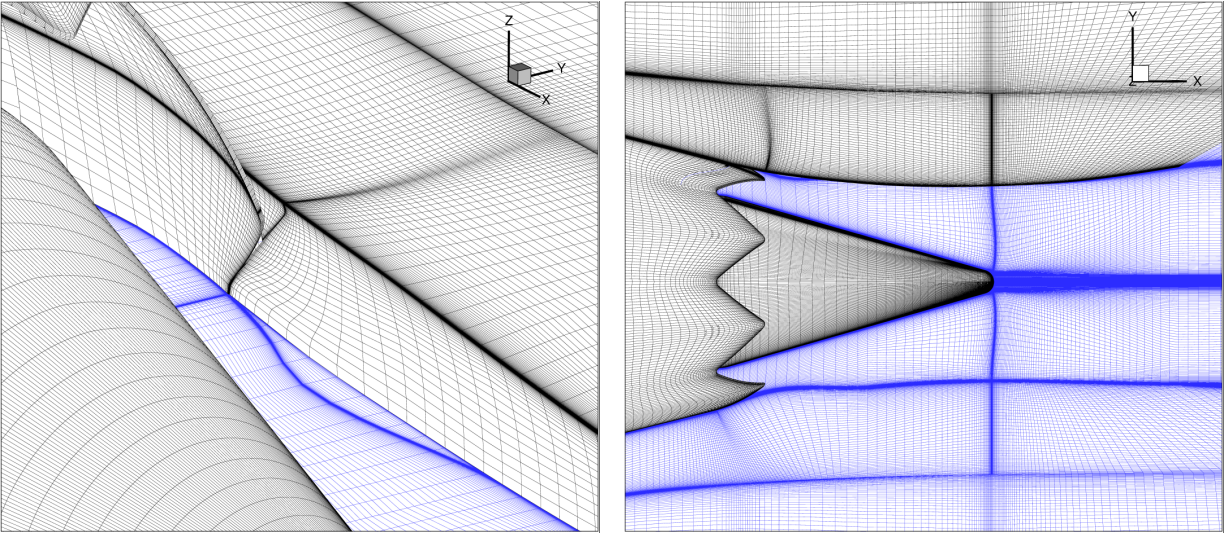


Figure 29: Case 5, Chevron Trough under Pylon: pylon grid interface views, with symmetry plane shown in blue.

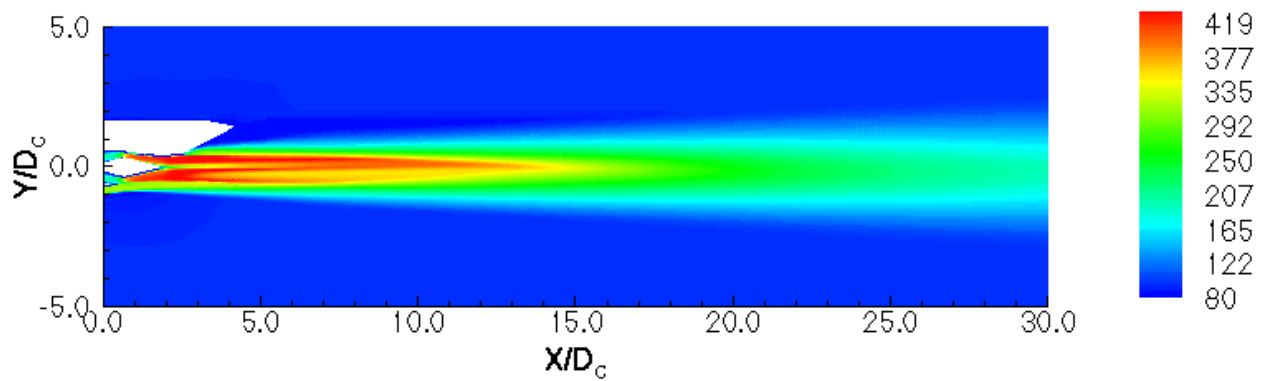


Figure 30: Case 5, Chevron Trough under Pylon Axial Velocity [m/s] contours.

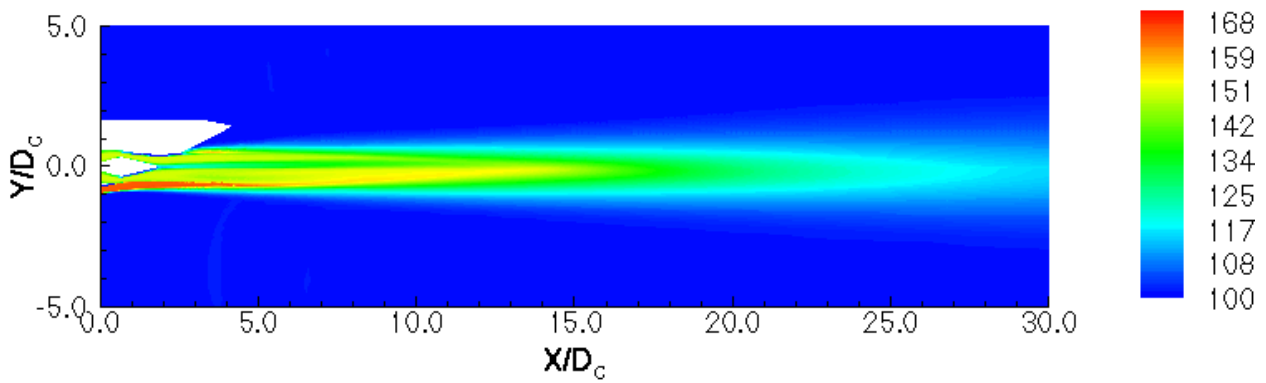


Figure 31: Case 5, Chevron Trough under Pylon: Total Pressure [kPa] contours.

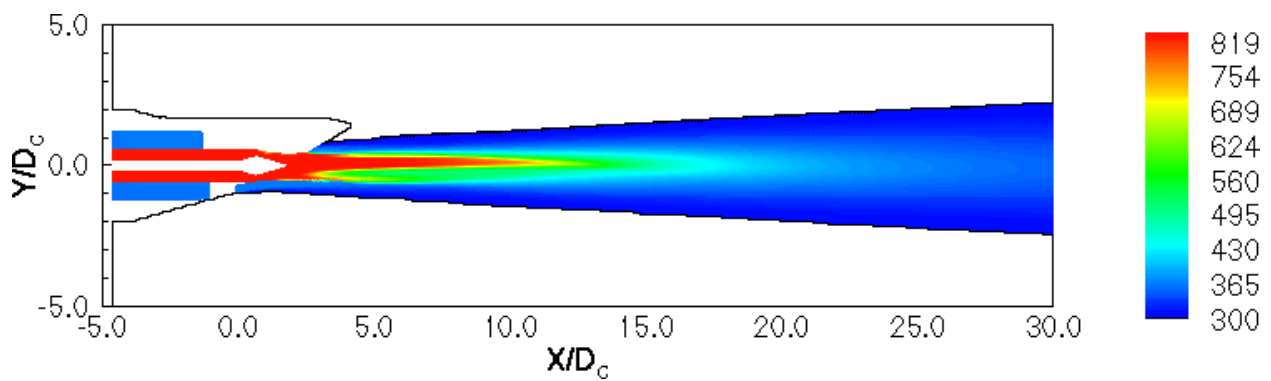


Figure 32: Case 5, Chevron Trough under Pylon: Total Temperature [K] contours.

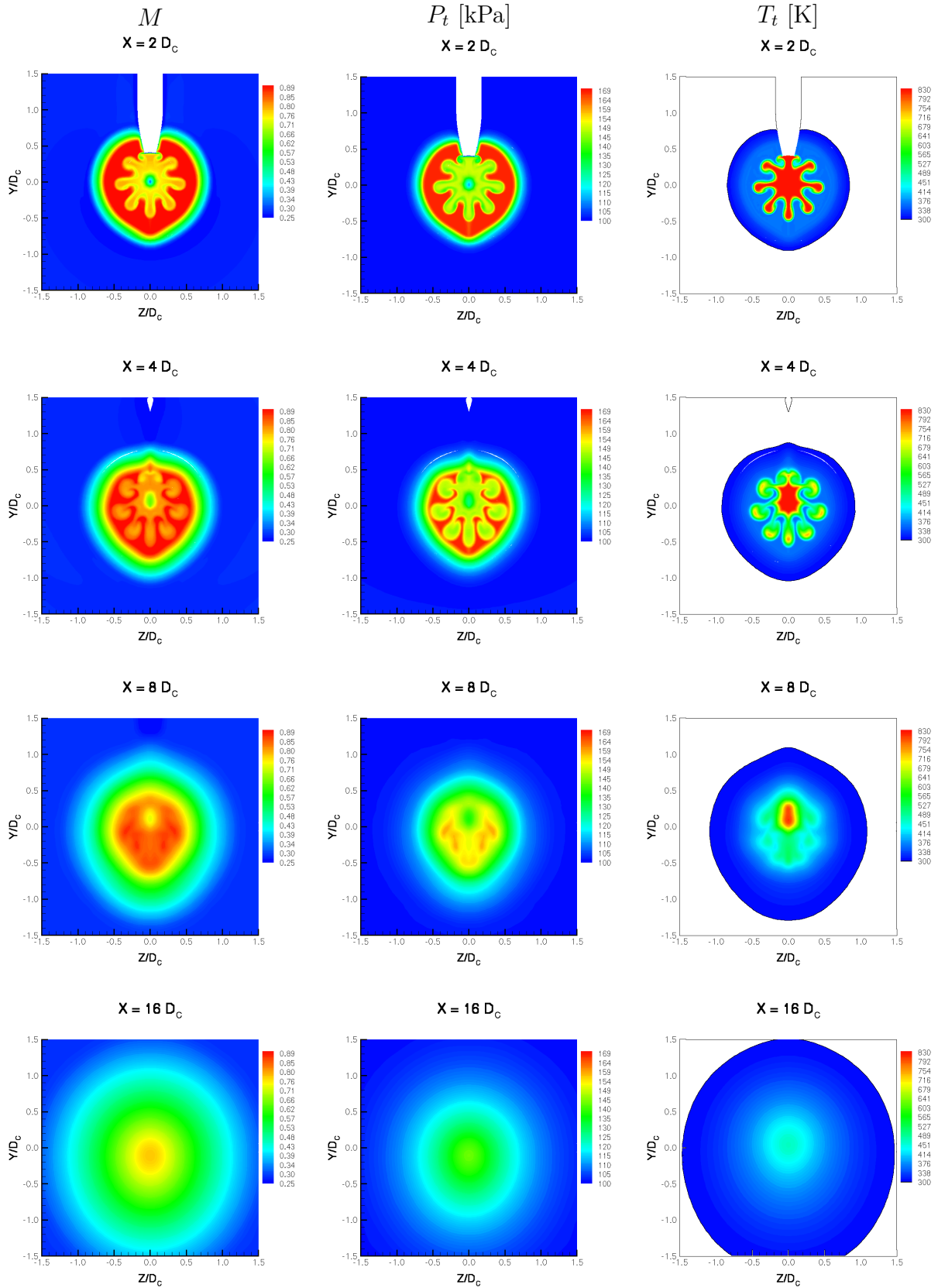


Figure 33: Case 5, Chevron Trough under Pylon: Mach number, Total Pressure[kPa] and Total Temperature [K] contours at stream-wise stations $x = 2, 4, 8, 16$ core diameters, starting from the fan exit.

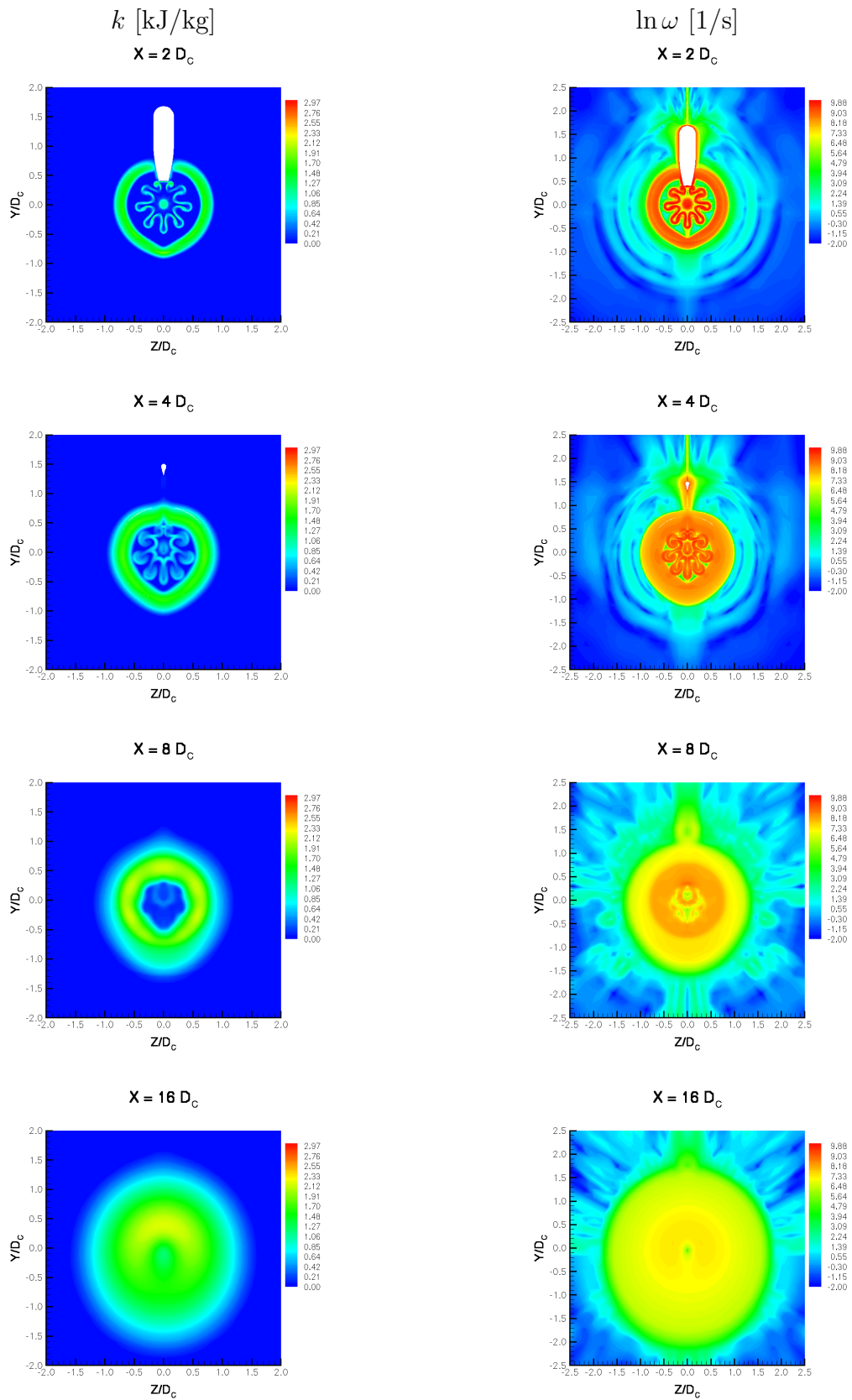


Figure 34: Case 5, Chevron Trough under Pylon: Specific Turbulence Kinetic Energy [kJ/kg] and Log Vorticity Magnitude [1/s] contours at stream-wise stations $x = 2, 4, 8, 16$ core diameters, starting from the fan exit.

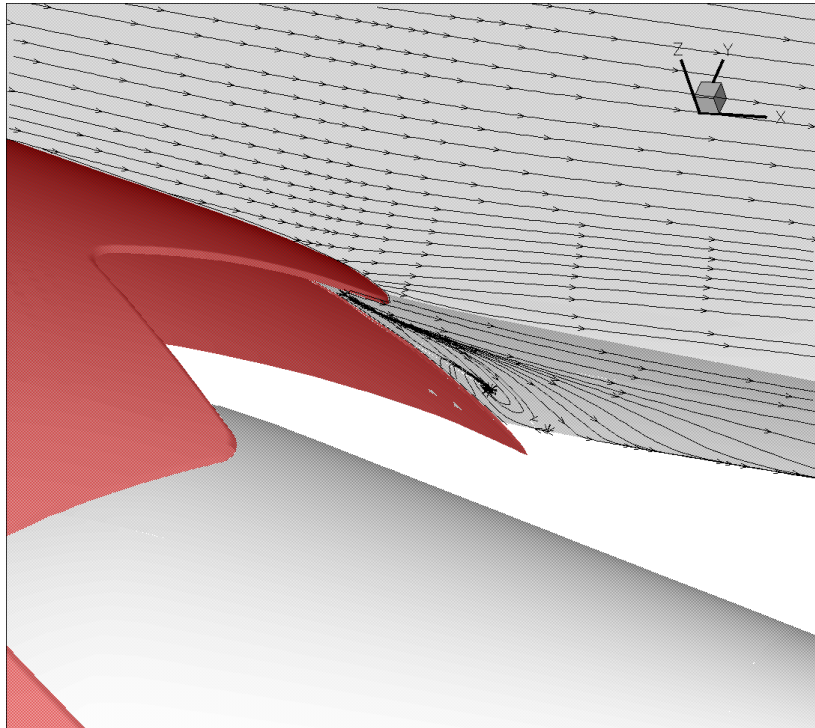


Figure 35: Case 4, Chevron Tip under Pylon: Pylon surface streamlines. Core nozzle shown in red.

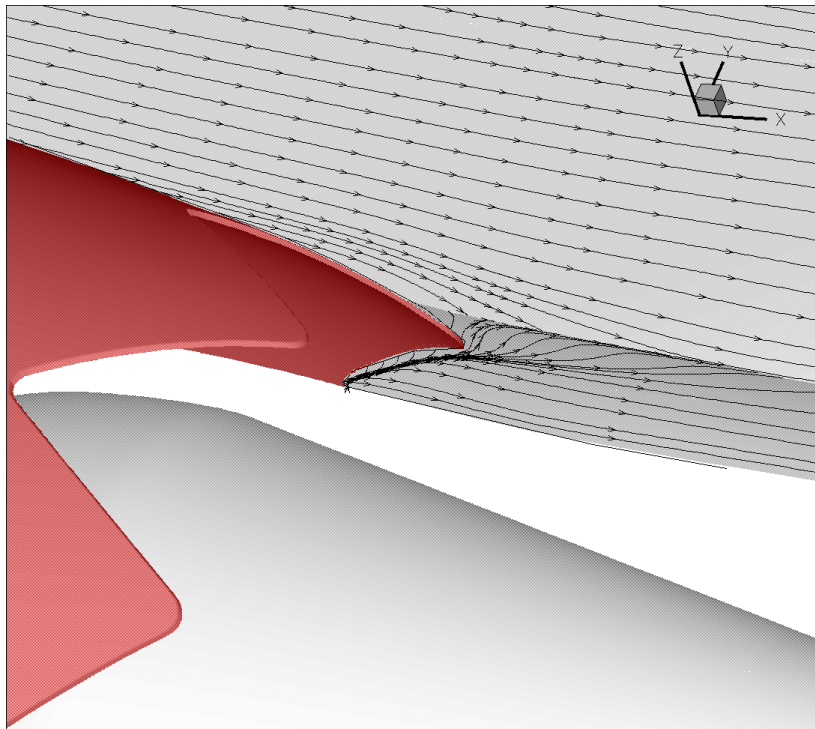


Figure 36: Case 5, Chevron Trough under Pylon: Pylon surface streamlines. Core nozzle shown in red.

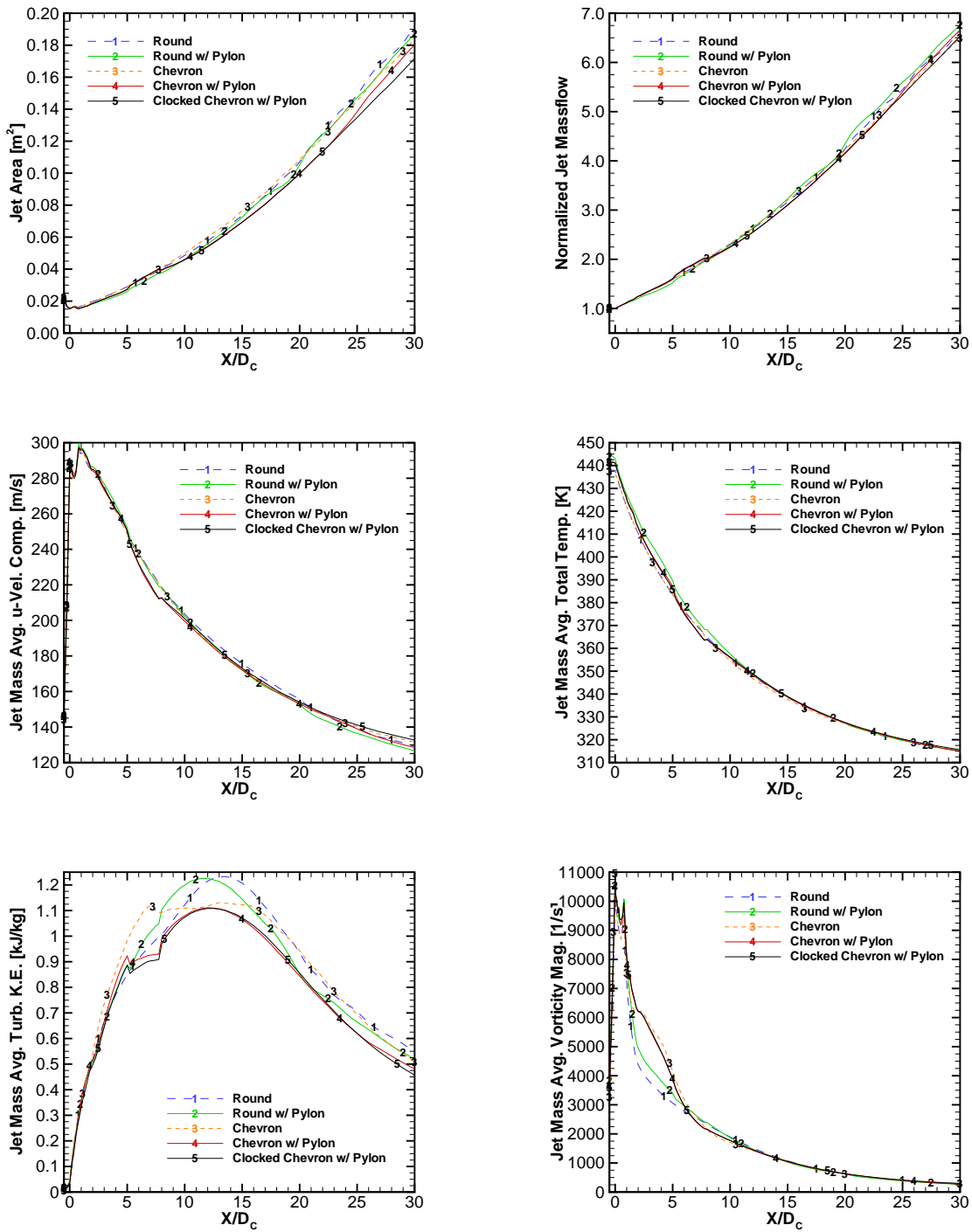


Figure 37: Full Jet: Axial distribution of Jet Area [m^2], Jet Mass, Mass Averaged Axial Velocity [m/s], Total Temperature [K], Specific Turbulence Kinetic Energy [kJ/kg] and Log Vorticity Magnitude [$1/s$].

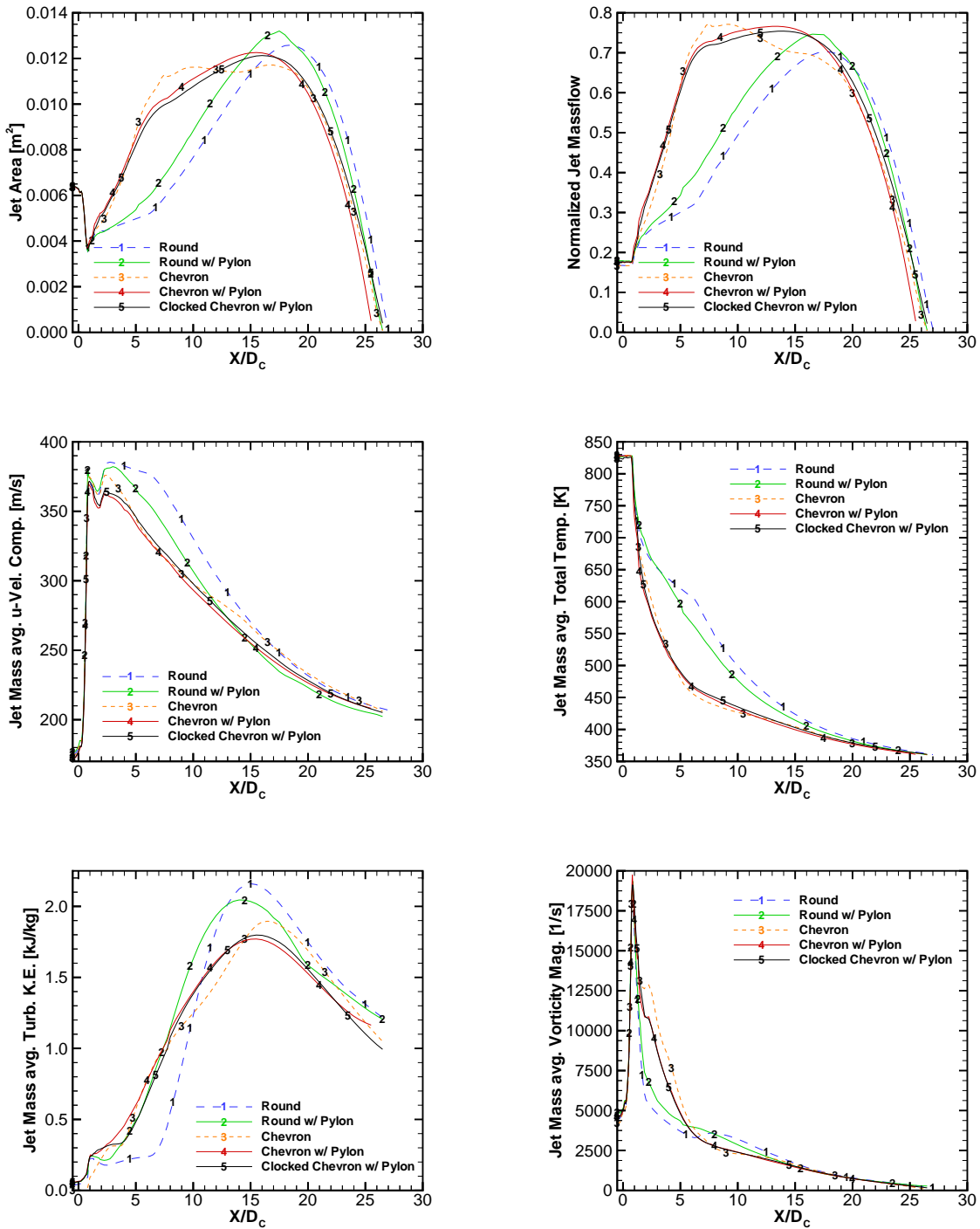


Figure 38: Core Jet: Axial distribution of Jet Area [m²], Jet Mass, Mass Averaged Axial Velocity [m/s], Total Temperature [K], Specific Turbulence Kinetic Energy [kJ/kg] and Log Vorticity Magnitude [1/s].

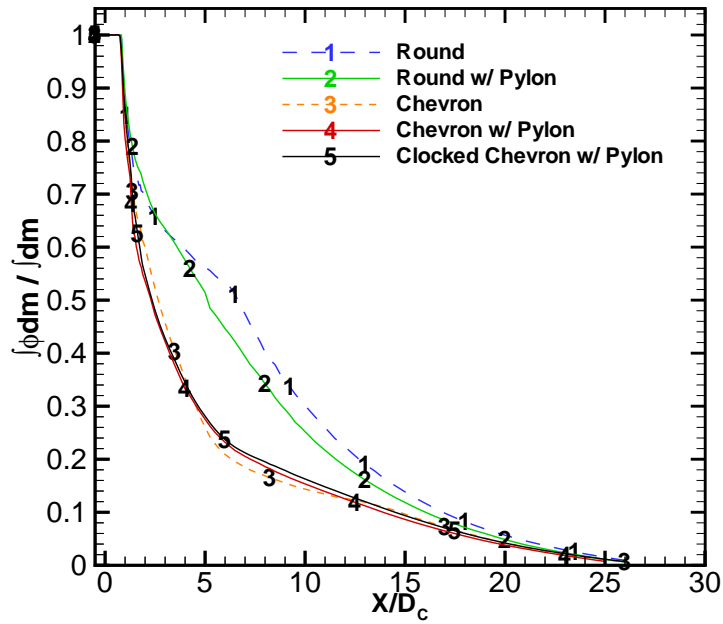


Figure 39: Mass averaged non-dimensional Total Temperature decay

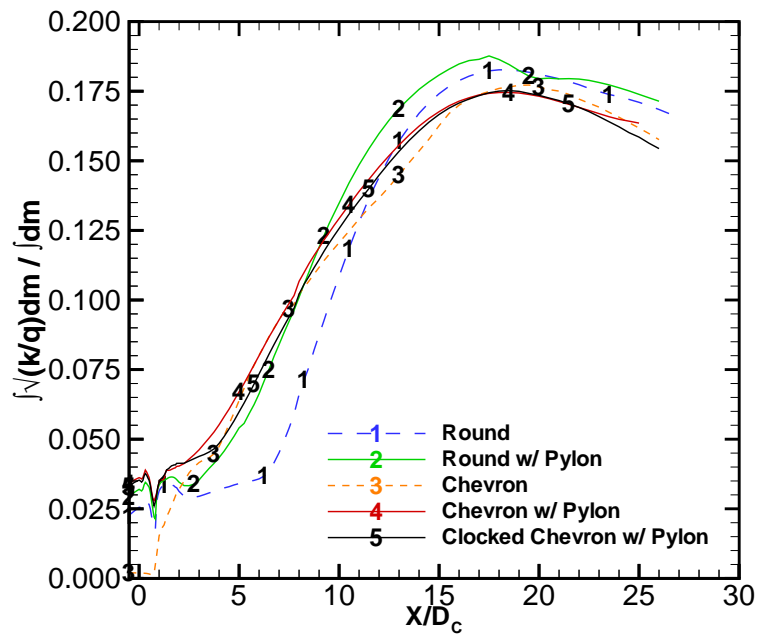


Figure 40: Mass averaged non-dimensional Turbulence Intensity decay

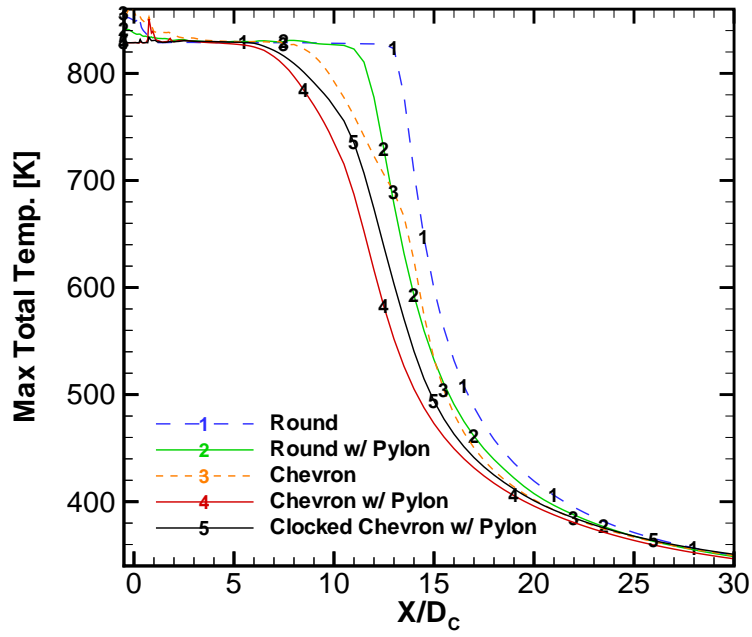


Figure 41: Axial distribution of maximum Total Temperature [K]

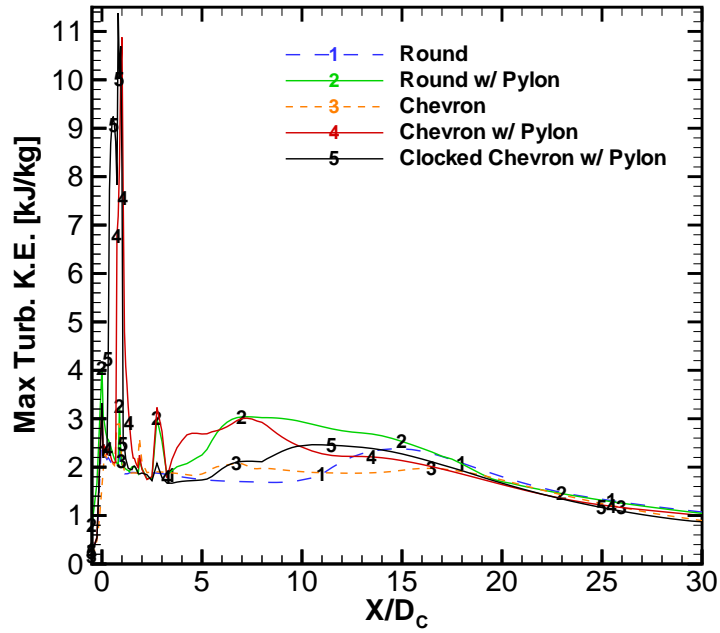


Figure 42: Axial distribution of maximum Specific Turbulence Kinetic Energy [kJ/kg]

REPORT DOCUMENTATION PAGE			Form Approved OMB No. 0704-0188
Public reporting burden for this collection of information is estimated to average 1 hour per response, including the time for reviewing instructions, searching existing data sources, gathering and maintaining the data needed, and completing and reviewing the collection of information. Send comments regarding this burden estimate or any other aspect of this collection of information, including suggestions for reducing this burden, to Washington Headquarters Services, Directorate for Information Operations and Reports, 1215 Jefferson Davis Highway, Suite 1204, Arlington, VA 22202-4302, and to the Office of Management and Budget, Paperwork Reduction Project (0704-0188), Washington, DC 20503.			
1. AGENCY USE ONLY (Leave blank)	2. REPORT DATE September 2001	3. REPORT TYPE AND DATES COVERED Contractor Report	
4. TITLE AND SUBTITLE Computational Analyses of Propulsion Aeroacoustics for Mixed Flow Nozzle Pylon Installation at Takeoff		5. FUNDING NUMBERS PO L-13395 WU 706-32-41-03	
6. AUTHOR(S) Steven J. Massey and Kenrick A. Waithe			
7. PERFORMING ORGANIZATION NAME(S) AND ADDRESS(ES) Eagle Aeronautics, Inc Hampton, VA Analytical Services and Materials, Inc. Hampton, VA		8. PERFORMING ORGANIZATION REPORT NUMBER	
9. SPONSORING/MONITORING AGENCY NAME(S) AND ADDRESS(ES) National Aeronautics and Space Administration Langley Research Center Hampton, VA 23681-2199		10. SPONSORING/MONITORING AGENCY REPORT NUMBER NASA/CR-2001-211056	
11. SUPPLEMENTARY NOTES Langley Technical Monitor: S. Paul Pao			
12a. DISTRIBUTION/AVAILABILITY STATEMENT Unclassified-Unlimited Subject Category 02 Distribution: Nonstandard Availability: NASA CASI (301) 621-0390		12b. DISTRIBUTION CODE	
13. ABSTRACT (Maximum 200 words) A CFD analyses is presented for a set of baseline and noise suppression mixed flow nozzles with and without a pylon installation. The five model configurations are as follows; a baselinecore/fan dual-stream nozzle with an external plug, a chevron mixer nozzle with a peak on the symmetry plane with external plug, both of the above nozzles with an installed bifurcatingpylon and lastly a clocked chevron mixer nozzle such that a trough is aligned with the center of the pylon. The fluid flow is simulated by solving the asymptotically steady, compressible, Reynolds-averaged Navier-Stokes equations using an implicit, up-wind, flux-difference splitting finite volume scheme and standard two equation k-epsilon turbulence model with a linear stress representation. All computations are performed using the multiblock, parallel, structuredcode PAB3D. Results indicate that the clocked chevron with pylon case achieves the most optimal levels of average and peak turbulence kinetic energy and vorticity and therefore is expected to be the quietest of the five configurations tested. Further study is required to refine expressions which are indicative of noise and mate these with rigorous noise prediction models.			
14. SUBJECT TERMS PAB3D; CFD; Aeroacoustics; Pylon; Chevron; PAA; QAT		15. NUMBER OF PAGES 35	
		16. PRICE CODE A03	
17. SECURITY CLASSIFICATION OF REPORT Unclassified	18. SECURITY CLASSIFICATION OF THIS PAGE Unclassified	19. SECURITY CLASSIFICATION OF ABSTRACT Unclassified	20. LIMITATION OF ABSTRACT UL